AD-761 179

EFFECT OF STRATOSPHERIC OZONE DEPLETION ON THE SOLAR ULTRAVIOLET RADIATION INCIDENT ON THE SURFACE OF THE EARTH

Pythagoras Cutchis

Institute for Defense Analyses

Prepared for:

Defense Advanced Research Projects Agency

March 1973

PAPER P-922

EFFECT OF STRATOSPHERIC OZONE DEPLETION ON THE SOLAR ULTRAVIOLET RADIATION INCIDENT ON THE SURFACE OF THE EARTH

Pythagoras Cutchis

March 1973

INSTITUTE FOR DEFENSE ANALYSES
SCIENCE AND TECHNOLOGY DIVISION

IDA Log No. HQ 72-14697
Copy 62 of 65 copies

47

The work reparted in this document wos conducted under Contract DAHC15 73 C 0200 for the Department of Defense. The publicotion of this IDA Poper does not indicate endorsement by the Department of Defense, nor should the contents be construed os reflecting the officiol position of thot ogency.

PAPER P-922

EFFECT OF STRATOSPHERIC OZONE DEPLETION ON THE SOLAR ULTRAVIOLET RADIATION INCIDENT ON THE SURFACE OF THE EARTH

Pythagoras Cutchis

March 1973

INSTITUTE FOR DEFENSE ANALYSES
SCIENCE AND TECHNOLOGY DIVISION
400 Army-Navy Drive, Arlington, Virginia 22202

Contract DAHC15 73 C 0200
Task T-90

IC

UNCLASSIFIED

Security Classification

DOCUMENT CONTROL DATA - R & D

(Security classification of title, body of abstract and indexing annotation must be entered when the overall report is classified)

1. ORIGINATING ACTIVITY (Corporate author)
INSTITUTE FOR DEFENSE ANALYSES
400 Army-Navy Drive
Arlington, Virginia 22202

2a. REPORT SECURITY CLASSIFICATION
UNCLASSIFIED

2b GROUP
--

3. REPORT TITLE
Effect of Stratospheric Ozone Depletion on the Solar Ultraviolet Radiation Incident on the Surface of the Earth

4. DESCRIPTIVE NOTES (Type of report and inclusive dates)
Paper P-922, March 1973

5. AUTHOR(S) (First name, middle initial, last name)
Pythagoras Cutchis

6. REPORT DATE	7a. TOTAL NO OF PAGES	7b. NO OF REFS
March 1973	40 ~~47~~	19

8a. CONTRACT OR GRANT NO	9a. ORIGINATOR'S REPORT NUMBER(S)
DAHC15 73 C 0200	P-922
b. PROJECT NO Task T-90	9b. OTHER REPORT NO(S) (Any other numbers that may be assigned this report) None
c	
d	

10. DISTRIBUTION STATEMENT
Approved for public release; distribution unlimited.

11. SUPPLEMENTARY NOTES	12. SPONSORING MILITARY ACTIVITY
N/A	Defense Advanced Research Projects Agency Arlington, Virginia 22209

13. ABSTRACT

Recent theoretical work indicates that the oxides of nitrogen that would be injected into the stratosphere by a fleet of supersonic transport aircraft could result in a significant depletion of natural stratospheric ozone. Since the stratospheric ozone layer shields the biosphere from harmful ultraviolet (UV) radiation, there is concern about the biological effects of the increase in UV radiation that would attend a reduction in the present amount of natural ozone. This paper estimates the factor by which UV radiation would be increased as a function of percentage ozone depletion and wavelength. To illustrate a potentially significant biological effect of increased UV radiation, the attendant increase in erythemal (sunburn-producing) UV radiation dosage is calculated for several conditions of ozone depletion, radiation wavelength, and solar zenith angle.

DD FORM 1 NOV 1473

UNCLASSIFIED

Security Classification

14 KEY WORDS	LINK A		LINK B		LINK C	
	ROLE	WT	ROLE	WT	ROLE	WT
solar ultraviolet radiation on surface of Earth						
atmospheric ozone depletion effect on solar UV radiation						
erythemal dose from solar UV radiation						

CONTENTS

I. INTRODUCTION

Recent theoretical research studies (e.g., Ref. 1) have indicated that the NO_x molecules that would be injected into the Earth's stratosphere by a hypothetical fleet of supersonic transport (SST) aircraft could result in a significant depletion of stratospheric ozone (Appendix). The highly absorbing ozone layer shields the biosphere from harmful solar ultraviolet (UV) radiation, and therefore there is legitimate concern about the biological effects of the increased UV radiation that would assuredly follow a reduction in the present amount of natural ozone. This paper does not attempt to independently assess the percentage of ozone depletion that may be expected but does estimate the factor of increase in UV radiation as a function of percentage ozone depletion and wavelength.

To determine the biological effect of increased UV radiation, it is necessary to know the action spectrum, i.e., the relative response of a biological specimen to UV radiation as a function of wavelength. The spectrum of erythemal or sunburn-producing action of UV radiation for Caucasian skin is well documented (Ref. 2), and hence it is used as an example in which the increase in erythemal dose to be expected is calculated. With this type of data as an input, it may be possible to obtain an estimate of the increase in the incidence of skin cancer that could be expected to result from a specified percentage reduction in the amount of stratospheric ozone.

II. OZONE DISTRIBUTION

The amount of ozone in a column of air increases significantly with latitude and also varies somewhat with longitude. At the higher latitudes, season of the year is an important factor. Over the Northern Hemisphere, the amount of total ozone is maximum in the spring and minimum in the fall, as can be seen in Figs. 1 and 2 (Ref. 3). The average values indicated on the contours should be multiplied by 10^{-3} to obtain values in atm-cm, which is the height of the resulting volume of ozone if all the ozone in the column of unit area were brought to normal surface pressure and temperature. Thus, in the middle of the USA, average total ozone increases from 0.28 atm-cm in the fall to 0.35 atm-cm in the spring, with smaller seasonal increases nearer the equator and larger seasonal increases nearer the North Pole. Higher latitudes receive much less solar UV radiation than the equator, because not only is the amount of total ozone greater but also the solar zenith angle θ is greater, which in effect increases the total ozone by sec θ.

There are daily fluctuations in the amount of total ozone, as can be seen from 1963 ozone measurements listed in Table 1 (Ref. 4). Daily fluctuations of as much as 20% in total ozone do not appear uncommon in spring, for example, in Colorado or Massachusetts. Daily UV radiation fluctuations at the surface of the Earth will be much larger, because ozone UV absorption is nonlinear with amount of ozone (Section VI), and in general the amount of cloud cover changes from day to day.

Monthly and annual variations in UV radiation are probably more significant with respect to biological effects. In Fig. 3, measurements at the Hamburg Meteorological Observatory (Ref. 5) indicate that

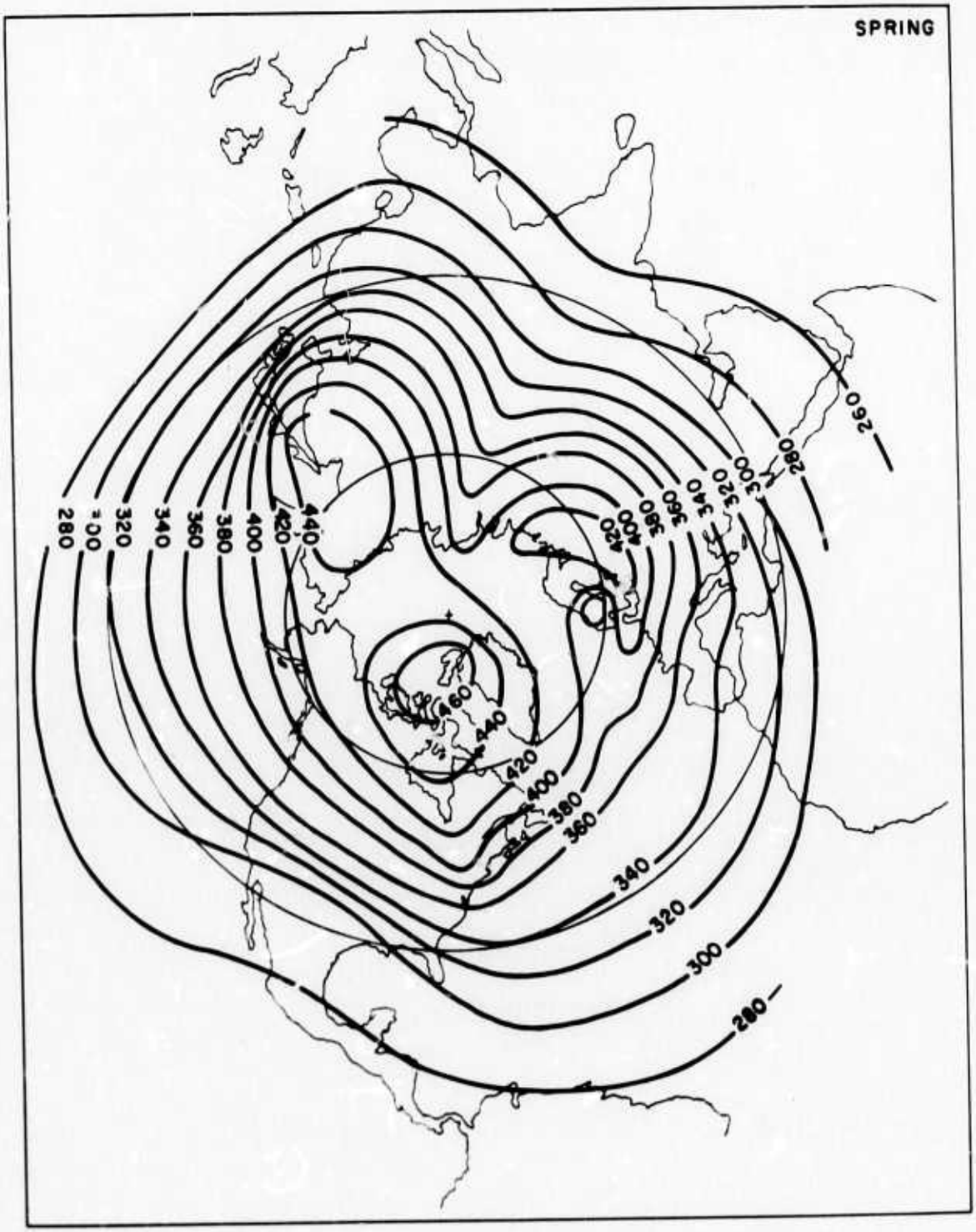

FIGURE 1. Average Distribution of Totol Ozone over the Northern Hemisphere in the Spring. (To convert contour values to atm-cm, multiply by 10^{-3}.) (Source: (Ref. 3.)

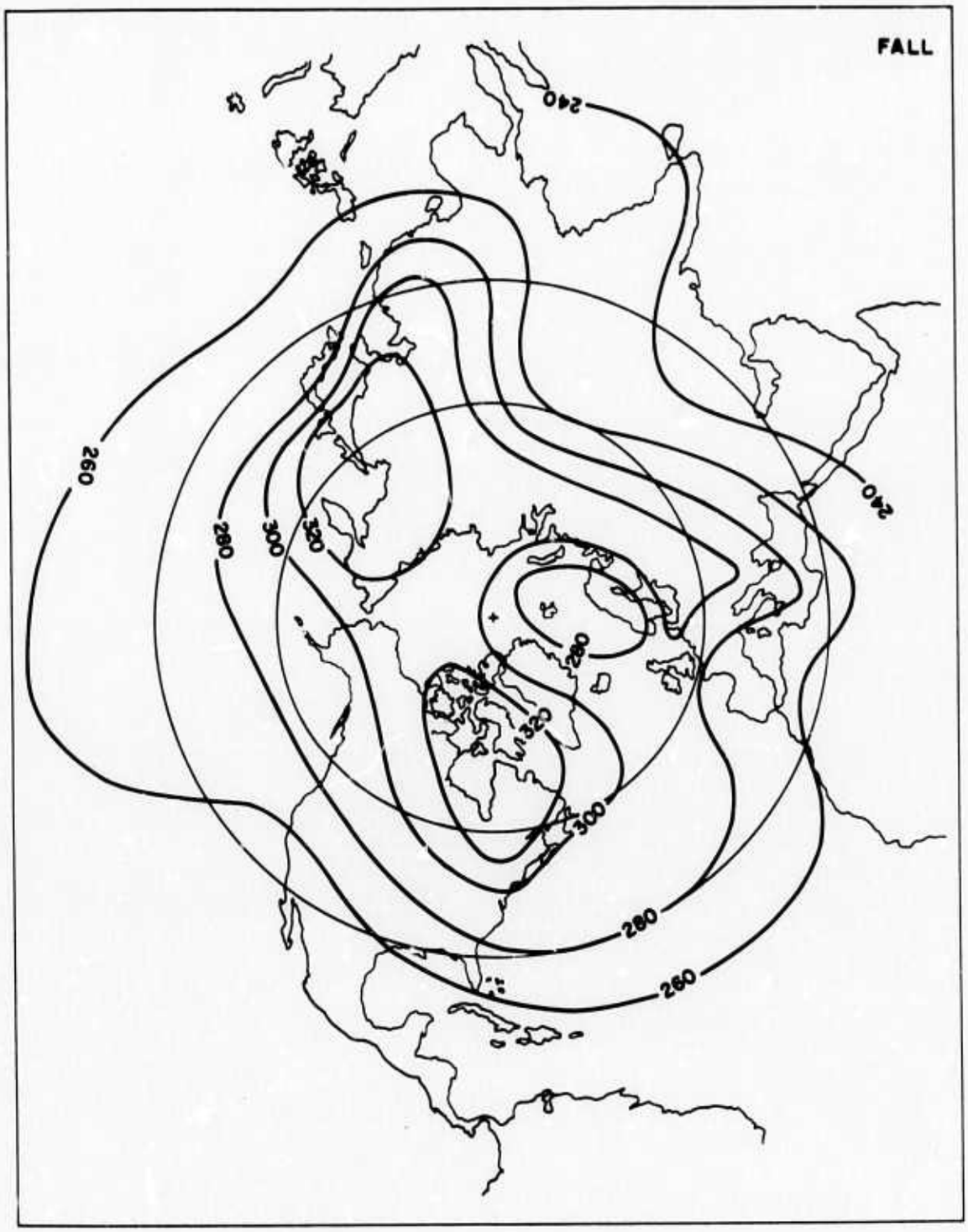

FIGURE 2. Average Distribution of Total Ozone over the Northern Hemisphere in the Fall. (To convert contour values to atm-cm, multiply by 10^{-3}.) (Source: Ref. 3.)

TABLE 1. 1963 OZONE MEASUREMENTS

(To convert values to atm-cm, multiply by 10^{-3}.)

Date	Canal Zone	N.M.	Col.	Bedford, Mass.	Churchill, Canada	Alaska	Thule	Wis.	Fla.	Seattle, Washington	Goose Bay
4-3	275	330	373	290	450	440	580				
4-4								392			
4-10		305		475					290		
4-17	275	290	302							375	470
4-24		340	410	495	450	450			295		448
4-29		350	337	410	480	450		392		420	446
4-30	275	350	332	390		450		440	300	400	421
5-1	275	350	404	400	475		440			475	490
5-2		350	440	480	440	400				475	397
5-3		325	390	450	465	400	475			450	373
5-4	274	320	316	400	460				325	420	
5-5		310	329	375					340	410	481
5-6		312	306	400	445			386	325	450	
5-7	264	310	310	425	445		430		320	460	465
5-8	274	308		395	460	450	456		330	460	463
5-9	264	295	293	375	460		462		325		494
5-10	264	292	300	380	470		462		300	440	
5-15	274	285	306	440	410		445		300	380	

Source: Ref. 4.

the maximum monthly mean of UV-B (280-315 nm) occurred in the month of July for 1955, 1956, and 1958, and in the month of June for 1957 and 1959. The July maximum of 1955 was 50% higher than the July maximum of 1958. Total UV-B radiation at Hamburg for the year 1955 was approximately 32% greater than for 1958.

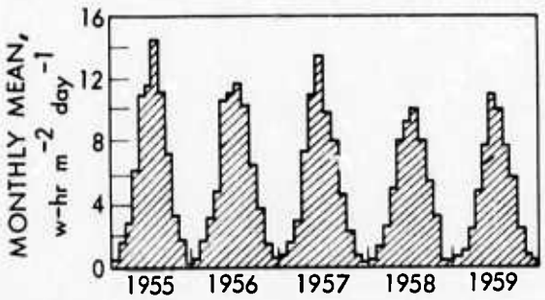

FIGURE 3. Annual Variation of UV-B (280-315 nm) Global Solar Radiation; Monthly Means at Hamburg, Germany, 1955-1959. (Source: Ref. 5.)

In Table 2, measured monthly means of total atmospheric ozone for the period 1925-1959 are tabulated (Ref. 6). From the data, it appears that the 2% difference in total ozone for July between 1955 and 1958 was not likely to have been the main reason for the Hamburg UV radiation differences in those years, but rather the variations in the amount of cloud cover. However, it is interesting to note that natural annual variations of 20% and greater in monthly means of total ozone have been recorded. In Ref. 6 it is suggested that total atmospheric ozone, through some unknown mechanism, is correlated with the sunspot cycle.

Ozone density over North America for March-April is shown in Fig. 4 (Ref. 3). Clearly, the distribution of ozone in altitude as well as the total amount of ozone varies with latitude. Thus, the density peaks at 24 km to 400 $\mu g\ m^{-3}$ at 12° N. latitude but peaks at 16 km to 700 $\mu g\ m^{-3}$ at 67° N. latitude. The altitude distribution of ozone is of significance in the calculation of scattered or diffuse sky UV radiation (Ref. 7).

TABLE 2. MONTHLY MEANS OF TOTAL ATMOSPHERIC OZONE, 1925-1959

(To convert values to atm-cm, multiply by 10^{-3}.)

Month		1925	26	27	28	29	30	31	32	33	34	35	36	37	38	39	40	41	42	43	44	45	46	47	48	49	50	51	52	53	54	55	56	57	58	59
	Val. *			360	328	285			298	344	332	320	303	312	318	327	352	348	368	339	275	300	268	270	334	314	310	332	366	316	328	298	314	304	312	335
Jan.	No. †			2	2	4			2	2	2	3	3	4	3	3	3	3	4	6	3	3	4	4	3	4	2	7	10	10	13	22	21	15	37	32
	Lat. ‡		52	45	45	30			39																											
	Val. *	424	333	370	346	305			332	354	342	370	335	352	325	327	383	399	406	355	371	362	318	366	314	330	342	380	367	355	369	343	335	338	353	342
Feb.	No. †	1	1	2	2	3			2	2	2	3	3	4	3	2	4	6	5	5	3	3	4	4	4	3	2	7	11	12	16	23	22	18	37	31
	Lat. ‡	52	52	45	45	29			39																											
	Val. *	382	347	400	367	302			356	370	370	355	387	353	332	362	394	416	397	376	380	371	355	372	339	344	346	410	424	371	379	346	340	328	366	356
Mar.	No. †	1	1	4	3	4			2	2	2	3	3	4	4	3	5	6	6	6	4	3	4	4	4	4	2	8	12	11	18	24	22	17	40	32
	Lat. ‡	52	52	51	47	30			39																											
	Val. *	424	358	402	379	319			358	356	342	362	385	337	365	357	404	407	398	381	378	396	351	382	378	368	367	388	406	388	400	341	352	340	371	364
Apr.	No. †	1	1	7	3	4			2	2	2	2	3	4	4	3	5	6	7	5	4	3	4	3	3	4	1	8	14	14	19	25	23	18	44	31
	Lat. ‡	52	52	53	47	30			39																											
	Val. *	403	375	395	378	301			338	360	344	358	365	320	344	363	374	396	382	369	362	382	308	362	378	363	360	385	398	379	281	346	333	343	355	345
May	No. †	1	1	7	3	4			2	2	2	2	3	4	4	3	6	5	6	6	4	3	4	3	4	3	1	9	14	13	20	24	22	18	44	31
	Lat. ‡	52	52	53	47	30			39																											
	Val. *	373	344	356	342	291			330	356	334	320	322	305	316	335	346	358	350	337	341	346	314	339	333	338	341	340	371	357	355	333	327	322	337	335
June	No. †	1	2	7	3	3			2	2	2	2	3	4	4	3	6	5	7	5	4	3	4	3	4	2	1	10	13	12	19	23	20	18	44	32
	Lat. ‡	52	52	53	47	30			39																											
	Val. *	364	314	338	314	268			314	319	317	314	316	285	298	314	326	331	332	360	318	308	295	322	310	310	311	328	341	337	341	316	307	319	321	318
July	No. †	1	5	7	3	4			2	2	2	3	3	4	4	3	6	5	6	5	4	3	4	3	4	2	1	11	14	13	21	27	20	34	47	33
	Lat. ‡	52	56	53	47	38			39																											
	Val. *	356	310	324	288	278	286	301	300	316	308	292	305	281	291	291	309	325	308	298	301	303	278	298	307	300	308	314	323	313	322	302	312	311	303	308
Aug.	No. †	1	4	7	3	4	1	1	2	2	2	3	3	4	4	3	5	6	6	5	4	3	4	3	4	2	2	10	14	13	20	26	19	35	45	33
	Lat. ‡	52	53	53	41	38	47	47	39																											
	Val. *	336	283	307	273	277		324	300	306	286	285	289	281	280	292	301	297	289	275	298	291	264	290	284	276	274	281	309	285	301	285	301	301	295	297
Sept.	No. †	1	5	7	6	1		1	2	2	2	3	3	4	4	4	5	5	6	5	3	2	4	3	4	2	2	11	12	12	21	26	17	34	44	34
	Lat. ‡	52	53	53	36	30		47	39																											
	Val. *	305	278	298	269	257		273	296	295	286	264	282	278	277	298	283	298	294	299	284	271	254	282	268	256	281	272	295	280	285	277	286	287	293	287
Oct.	No. †	1	4	5	6	1		1	2	2	2	3	4	4	3	4	4	6	5	5	4	3	4	3	4	2	2	10	12	12	22	24	17	35	44	33
	Lat. ‡	52	51	51	36	30		47	39																											
	Val. *	295	286	274	266			277	292	290	275	277	271	262	288	290	283	291	290	281	283	248	248	251	252	278	298	273	280	265	283	274	276	288	296	296
Nov.	No. †	1	1	2	5			1	2	2	2	3	3	4	2	4	5	6	4	5	4	4	4	3	4	2	5	10	11	10	18	22	18	38	43	31
	Lat. ‡	52	47	45	34			47	39																											
	Val. *		313	310	282			291	285	320	273	288	284	296	288	276	297	305	275	280	276	256	281	262	309	294	316	323	322	299	290	286	283	286	313	315
Dec.	No. †		1	2	5			1	2	2	3	3	3	4	1	4	4	5	4	4	4	4	3	3	3	2	6	10	11	8	17	20	16	31	40	31
	Lat. ‡		47	45	34			47	39																											
	Val. *	366	322	344	319	288	286	293	317	332	317	317	320	305	310	319	338	348	341	329	322	320	294	316	316	316	321	336	350	329	328	312	314	314	326	325
Aver-	No †	10	26	59	44	32	1	5	24	24	25	33	37	48	40	39	58	64	66	62	45	37	47	39	49	32	27	111	148	140	224	286	237	314	509	384
age	Lat. ‡	52	52	50	42	31	47	47	39																											

* Monthly or annual ozone value.

† Number of stations included in monthly or annual value.

‡ Average latitude of all stations contributing to average value.

Source: Ref. 6.

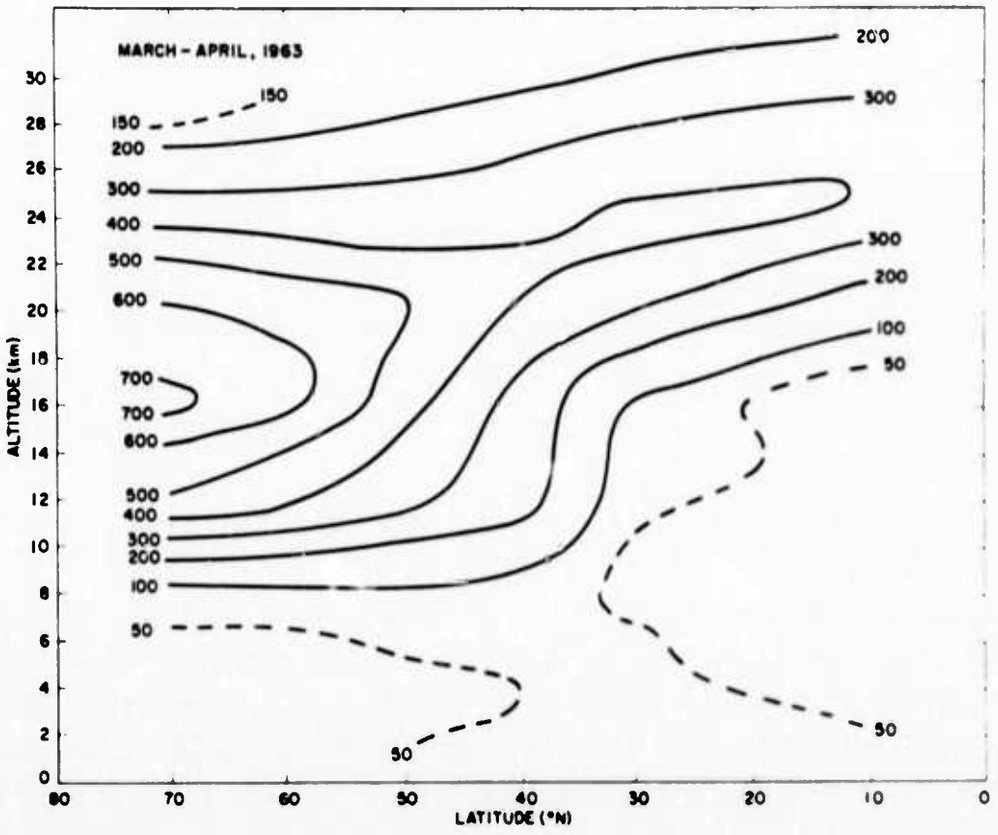

FIGURE 4. Average Ozone Density over the North American Continent Derived from Ozonesonde Network Data, March-April 1963. (Contour values are in $\mu g\ m^{-3}$.) (Source: Ref. 3.)

From the above discussion it may be concluded that natural forces induce sizable variations in the ozone layer over both short and long time periods. While some comfort can be derived from the fact that no adverse biological effects are known to have been attributable to these natural variations, it is important to recognize that any unnatural (i.e., man-made) depletion of stratospheric ozone would be a unidirectional variation, not a cyclical one. Thus, all daily, monthly and annual means of natural UV radiation would be increased by such an ozone depletion with the distinct possiblility of attendant adverse biological effects.

III. OZONE ULTRAVIOLET ABSORPTION

If x is the amount of total ozone in atm-cm to be traversed by a beam of incident UV radiation of wavelength λ and intensity $I_0(\lambda)$, the residual intensity $I(\lambda, x)$ in the beam is given by

$$I(\lambda, x) = I_0(\lambda)\, e^{-xA(\lambda)}, \tag{1}$$

where $A(\lambda)$ is the ozone absorption coefficient in $(\text{atm-cm})^{-1}$ STP, which varies strongly with λ, as shown in Fig. 5 (Refs. 3, 8, 9). In the wavelength region of most concern from a biological impact standpoint, 280 nm $< \lambda <$ 320 nm, the linear behavior of A on a semi-log plot permits one to express A as an exponential function of λ, i.e.,

$$A(\lambda) = k_1\, e^{-k_2\lambda}, \tag{2}$$

where k_1 and k_2 are constants.

Substituting Eq. 2 in Eq. 1, one obtains

$$I(\lambda, x) = I_0(\lambda)\, e^{-k_1 x e^{-k_2\lambda}} \tag{3}$$

$$(280 \text{ nm} < \lambda < 320 \text{ nm})$$

which explains the extremely sharp cutoff that the ozone layer provides in shielding the surface of the Earth from biologically harmful UV radiation of wavelengths less than ~ 300 nm. For this reason, solar UV radiation below 300 nm is extremely difficult to measure on

the surface of the Earth. At Davos, Switzerland, at an elevation of 1590 m, UV radiation at 297.5 nm has been measured (Ref. 10), but any attempt to obtain spectral measurements much below that wavelength would quickly encounter severe instrumentation problems.

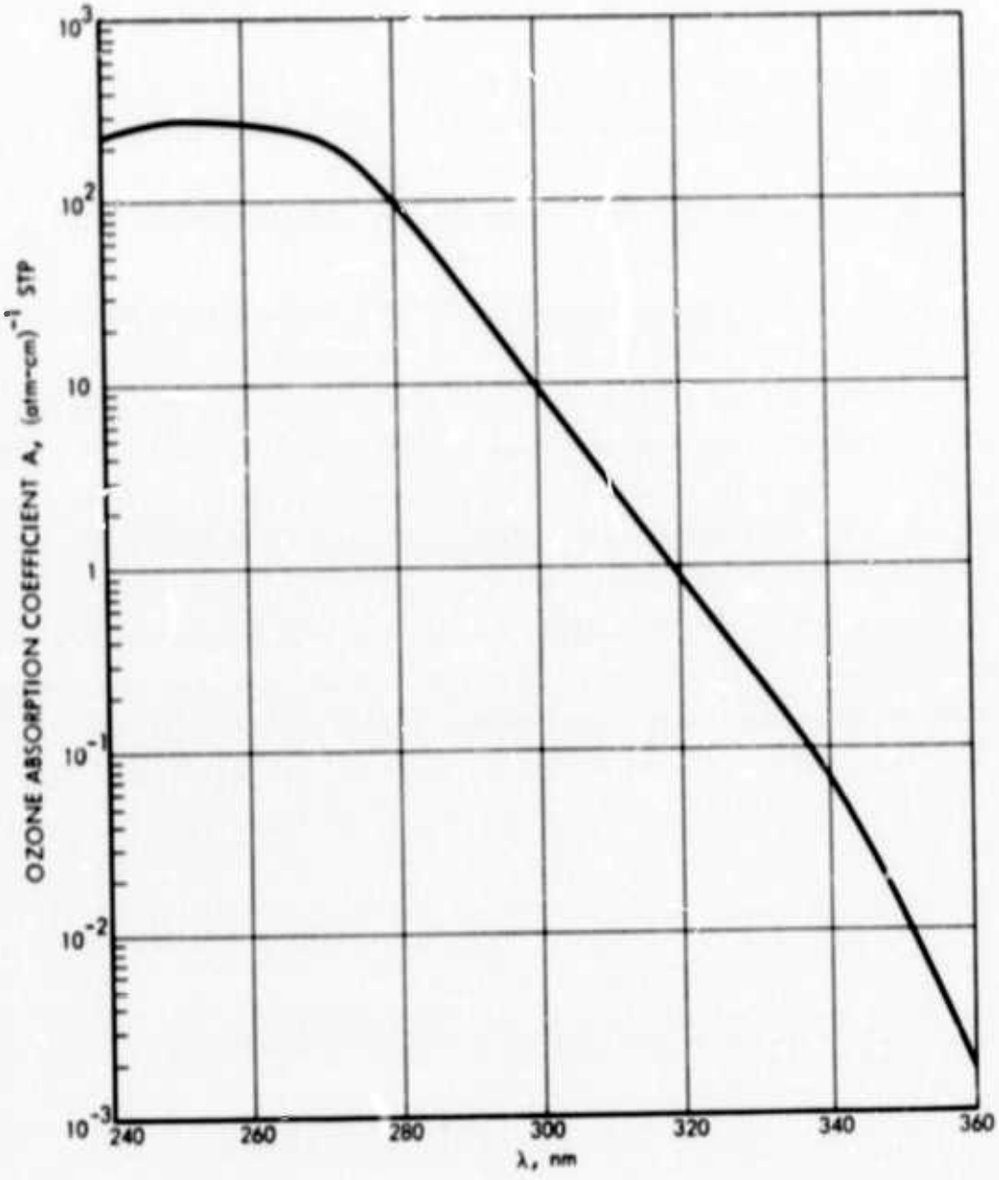

FIGURE 5. Ozone Absorption Coefficient. (Source: Refs. 3,8,9.)

IV. SOLAR ULTRAVIOLET IRRADIANCE

Only 2.2% of the solar constant is associated with UV wavelengths below 320 nm and only 1% with UV wavelengths below 300 nm, but this energy, in combination with the protective atmospheric blanket, has had a major impact on the evolution of life on Earth. It has been demonstrated that ultraviolet radiation affects DNA, RNA, and protein synthesis (Refs. 11 and 12). In Fig. 6 the solar spectral irradiance $H_{\Delta\lambda}$ is plotted as a function of λ for zero air mass (i.e., outside the Earth's atmosphere), as obtained from tabular information in Ref. 13. Values above 300 nm were measured by the National Aeronautics and Space Administration (NASA) from a research airplane flying at 38,000 ft. Data from Ref. 14 were used for the range from 260 to 300 nm, and rocket data of the Naval Research Laboratory (Ref. 15) were used for wavelengths below 260 nm. The absolute accuracy of this NASA solar spectral irradiance curve appears better than 10% on the basis of NASA comparisons with data collected by previous investigators; such accuracy is more than adequate for the purposes of this paper.

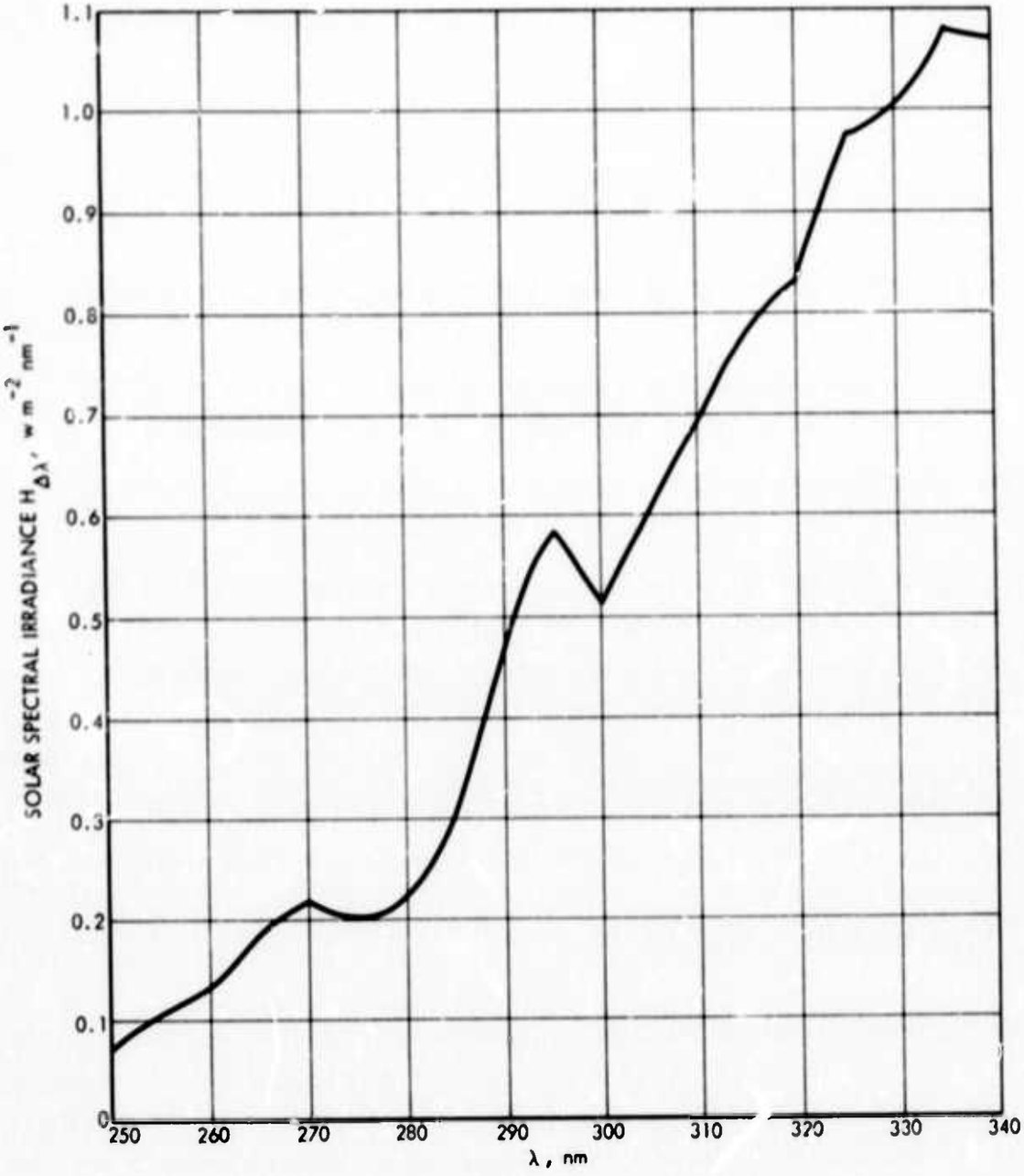

FIGURE 6. Solor Spectral Irradiance for Zero Air Mass in the Ultroviolet. (NASA proposed standord curve, from Ref. 13.)

V. SOLAR ULTRAVIOLET RADIATION INCIDENT ON THE SURFACE OF THE EARTH

There are two components of the solar UV radiation that is incident on the surface of the Earth:

1. The direct solar radiation subtending the sun and attenuated by atmospheric scattering and absorption, and
2. Scattered or diffuse sky radiation emitted by the atmosphere itself and subtending some 2π steradians in open spaces.

The calculation of the direct solar radiation is a relatively straightforward problem, but the calculation of the scattered radiation fluxes due to all orders of scattering in the ozone absorption bands was not mathematically solved until 1966, by Dave and Furukawa (Ref. 7).

The direct solar radiation flux on a surface normal to the incident direction, assuming a flat-Earth approximation,* is given by

$$I(\lambda, x, \theta) = I_0(\lambda)\, e^{-A(\lambda) \times \sec\theta - \tau_r(\lambda) \sec\theta}, \qquad (4)$$

where τ_r is the Rayleigh scattering optical thickness. There is yet another attenuation due to aerosol scattering, but this was not included in the calculations which were made in Ref. 7 and which will be used in this paper. For a model clear standard atmosphere, a zenith angle θ of 60°, and a wavelength of 300 nm, the aerosol transmission coefficient would be $e^{-0.52}$ or 0.60 (Ref. 3). Obviously, in locales with a smog-laden atmosphere, direct solar UV radiation will be more attenuated; on the other hand, diffuse sky radiation will be increased.

*Very good approximation for $\theta < 75^\circ$.

The direct and scattered solar radiation fluxes on a horizontal surface for π units per unit area normal to the incident direction are tabulated in Ref. 7 as functions of wavelength, solar elevation, and pressure level. A single distribution of ozone with a total amount of 0.341 atm-cm of ozone (Fig. 7) was used in the computer program. Five values of solar zenith angle θ (0°, 30°, 60°, 75°, and 85°), 16 wavelengths (5 nm apart in the 287.5- to 322.5-nm region), and 20 pressure levels were selected. The only pressure level discussed here is 1000 mb (i.e., sea level).

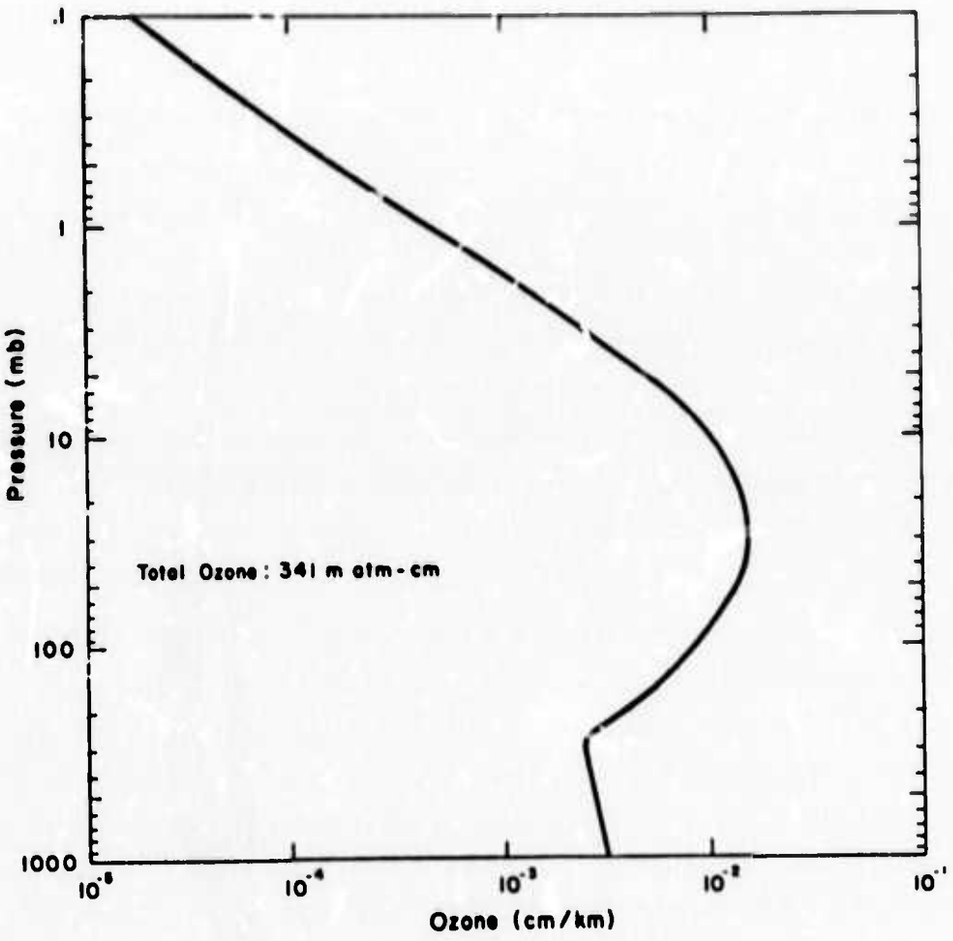

FIGURE 7. The Vertical Distribution of Ozone Used in the Model Atmosphere of Ref. 7.

By multiplying the tabulated flux values in Ref. 7 by the solar irradiance values from Fig. 6 and dividing by π, Figs. 8-11 were obtained for direct solar UV irradiance and scattered UV irradiance (and their sum) on a sea-level horizontal surface for 0.341 atm-cm of total ozone and zenith angles of 0°, 30°, 60°, and 75°, respectively. Note that, for zenith angles of 30° and below, the direct solar irradiance exceeds the scattered, and that from about 30° upwards the scattered irradiance is predominant. As expected from the behavior of the ozone absorption coefficient, the irradiance falls off precipitously below 300 nm, necessitating a second logarithmic ordinate scale on the left for these lower wavelengths. Also to be noted is the sharp decrease in irradiance for solar zenith angles greater than 60°.

The zenith-angle dependence of UV irradiance translates into a time dependence at any locale with a noon peak whose magnitude depends on latitude and time of year. The variation of global (direct solar plus scattered) UV irradiation with time of day, latitude, and season is illustrated in Fig. 12 (Ref. 5) for λ = 307.5 nm, the wavelength at which the erythemal dose curve peaks (Section VI and Fig. 14). The curves of Fig. 12 are instructive in describing the variations of worldwide solar UV irradiation at 307.5 nm, but their accuracy is open to question inasmuch as they are not based on the Dave-Furukawa formulas for the determination of scattered radiation.

Assuming cloudless days, Table 3 shows the monthly sums of UV radiation at 307.5 nm as computed in Ref. 5 for each month of the year for all latitudes in 10° increments. The influence of clouds on UV-B global solar radiation, according to Büttner (Ref. 16), is shown in Fig. 13. The results of Table 3 can be considered only approximate, since, among other things, there is no longitudinal variation, which Figs. 1 and 2 indicate there must be.

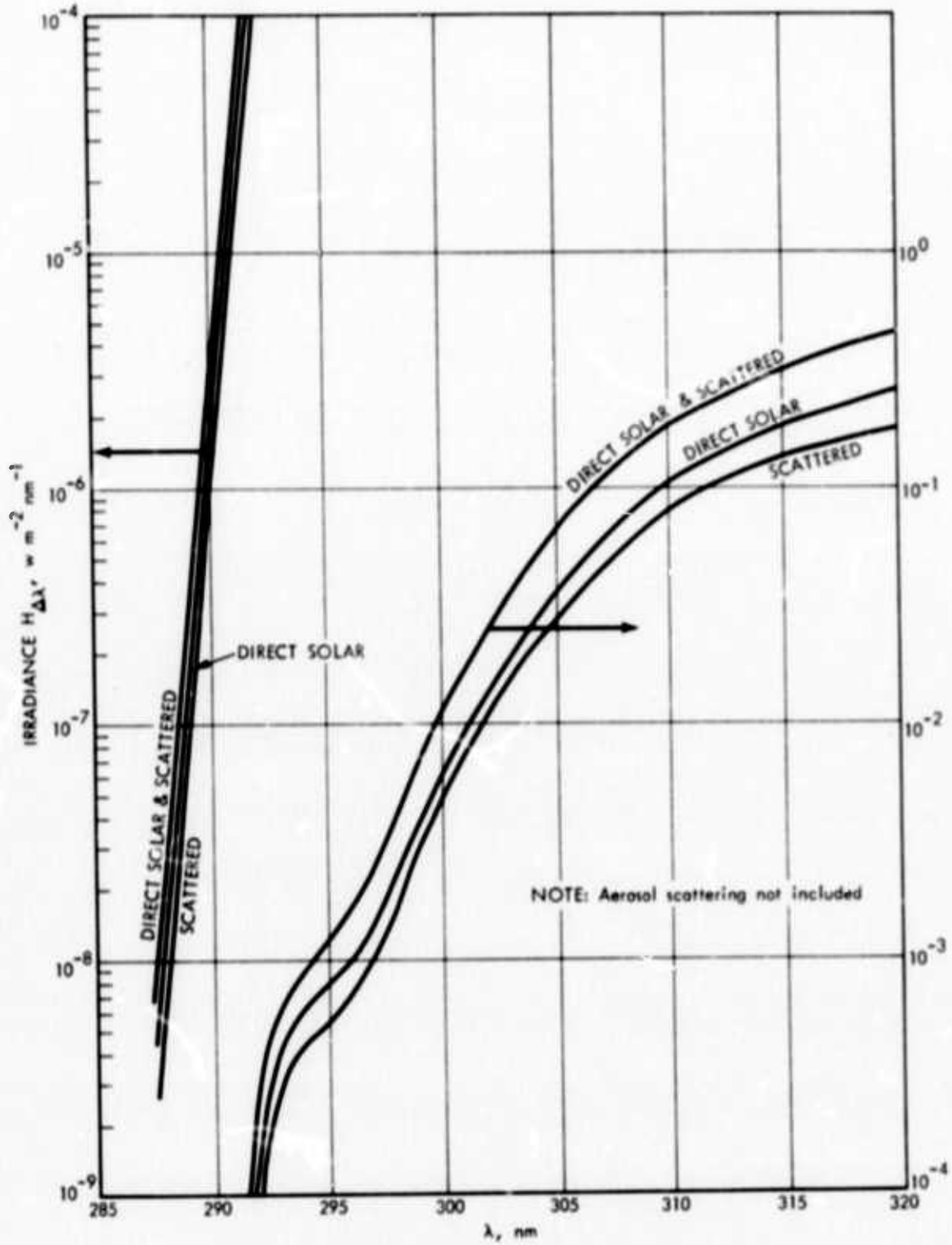

FIGURE 8. Direct Solar UV Irradiance and Scattered UV Irradiance on a Horizontal Surface at Sea Level for Solar Zenith Angle θ of [illegible] and 0.341 atm-cm of Total Ozone. (Data Source: Ref. 7.)

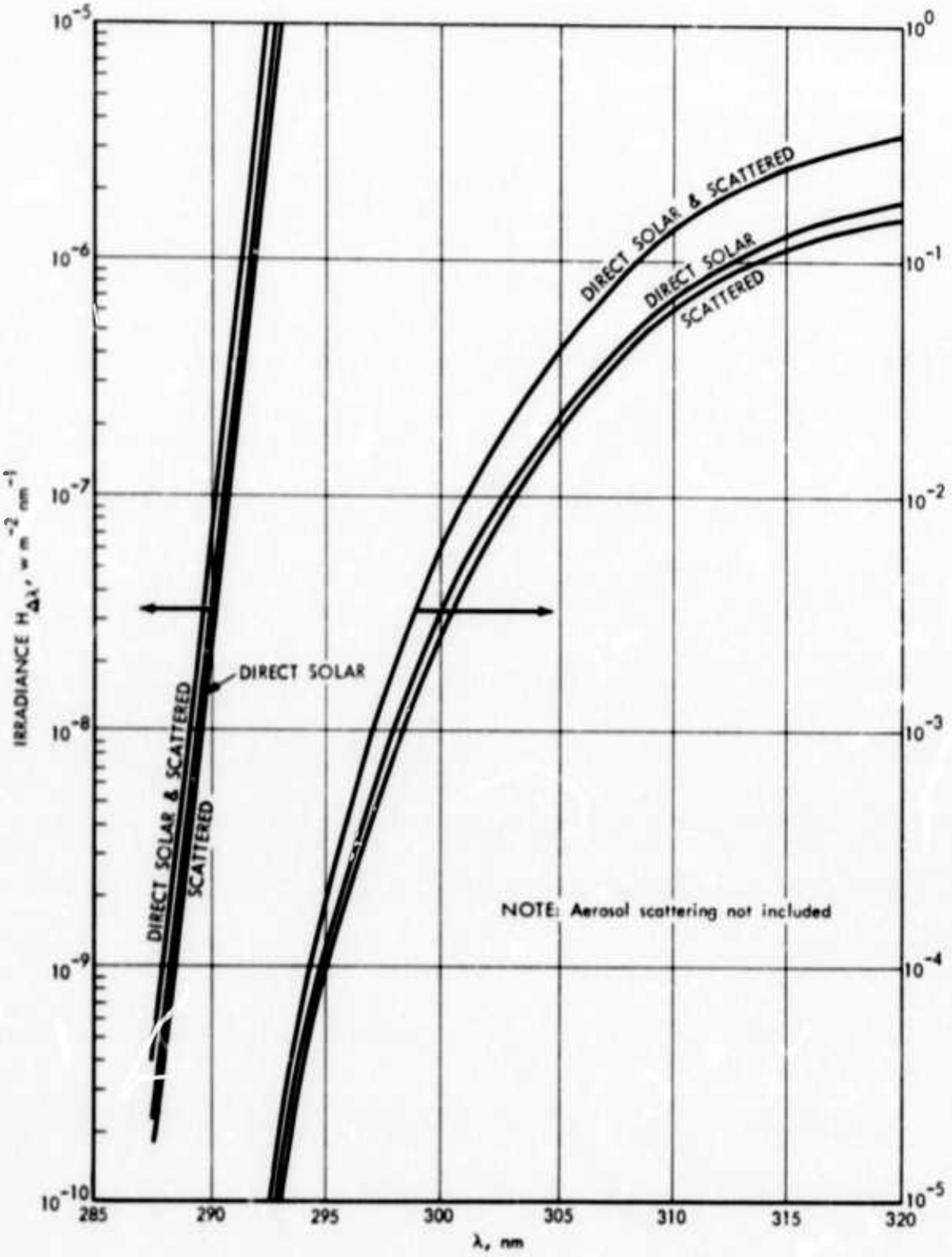

FIGURE 9. Direct Solor UV Irradiance ond Scottered UV Irradiance on o Horizontol Surface ot Seo Level for Solar Zenith Angle θ of 30° ond 0.341 atm-cm of Total Ozone. (Data Source: Ref. 7.)

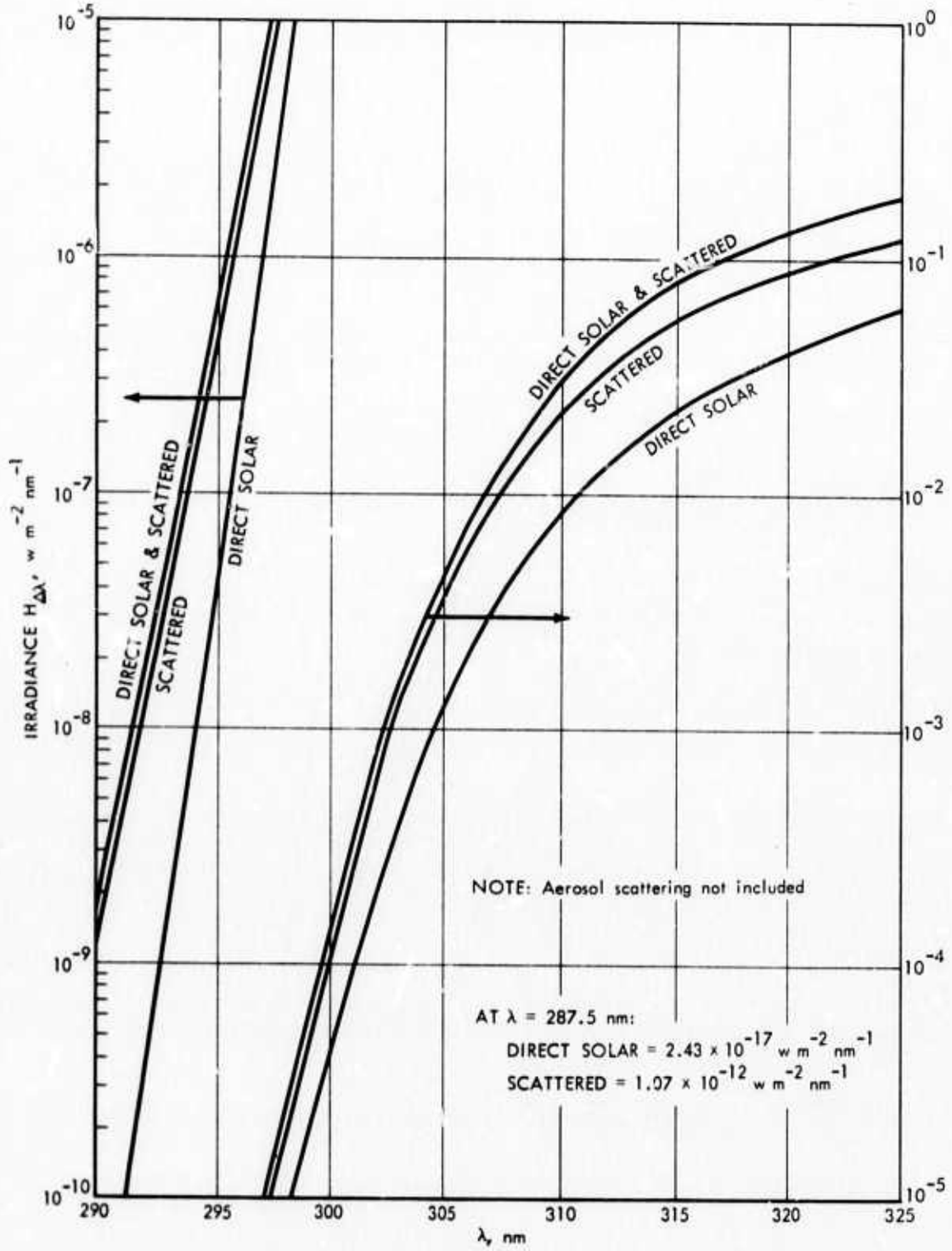

FIGURE 10. Direct Solar UV Irradiance and Scattered UV Irradiance on a Horizontal Surface at Sea Level for Solar Zenith Angle θ of 60° and 0.341 atm-cm of Total Ozone. (Data Source: Ref. 7.)

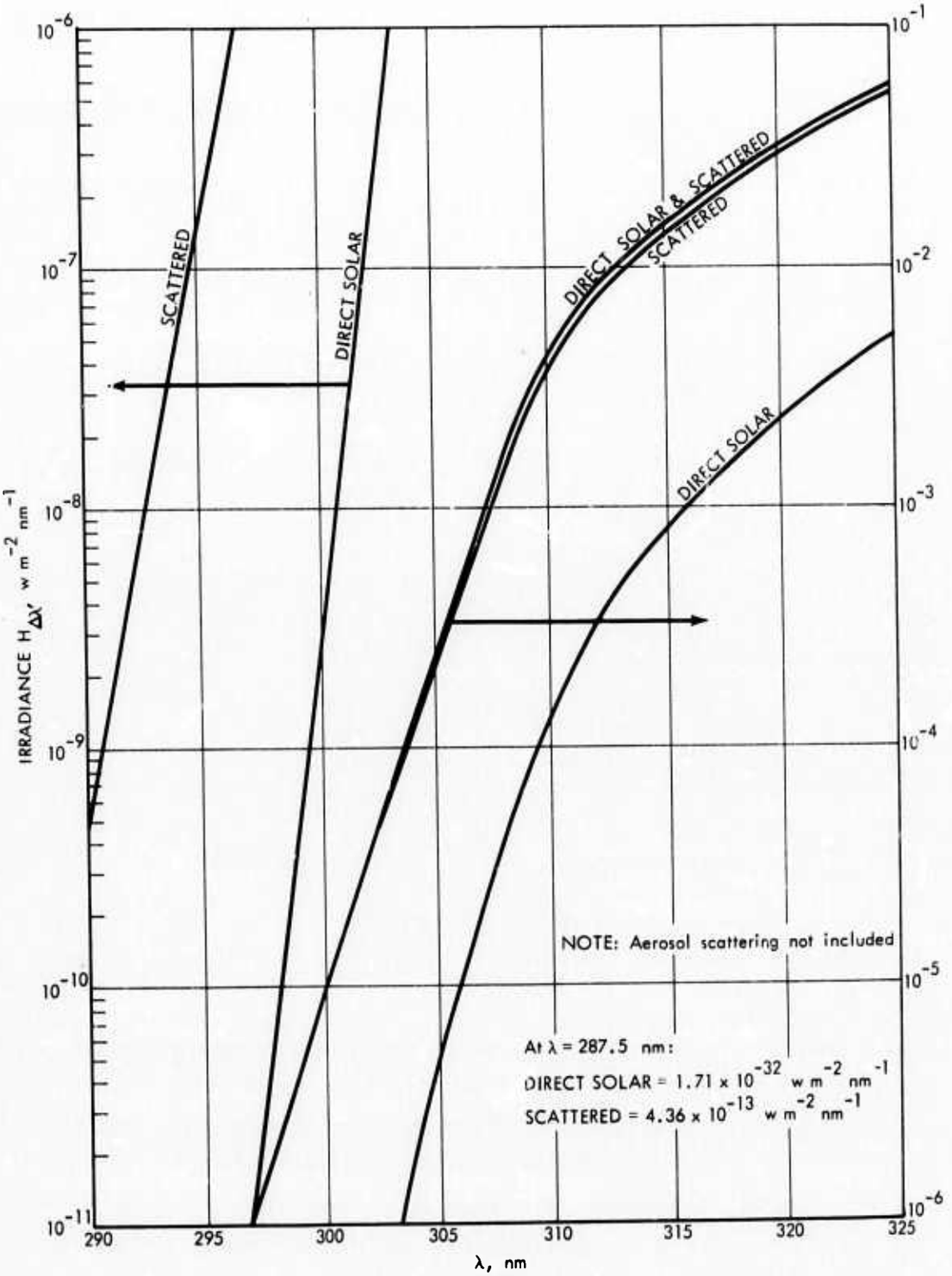

FIGURE 11. Direct Solar UV Irradiance and Scattered UV Irradiance on a Horizontal Surface at Sea Level for Solar Zenith Angle θ of 75° and 0.341 atm-cm of Total Ozone. (Data Source: Ref. 7.)

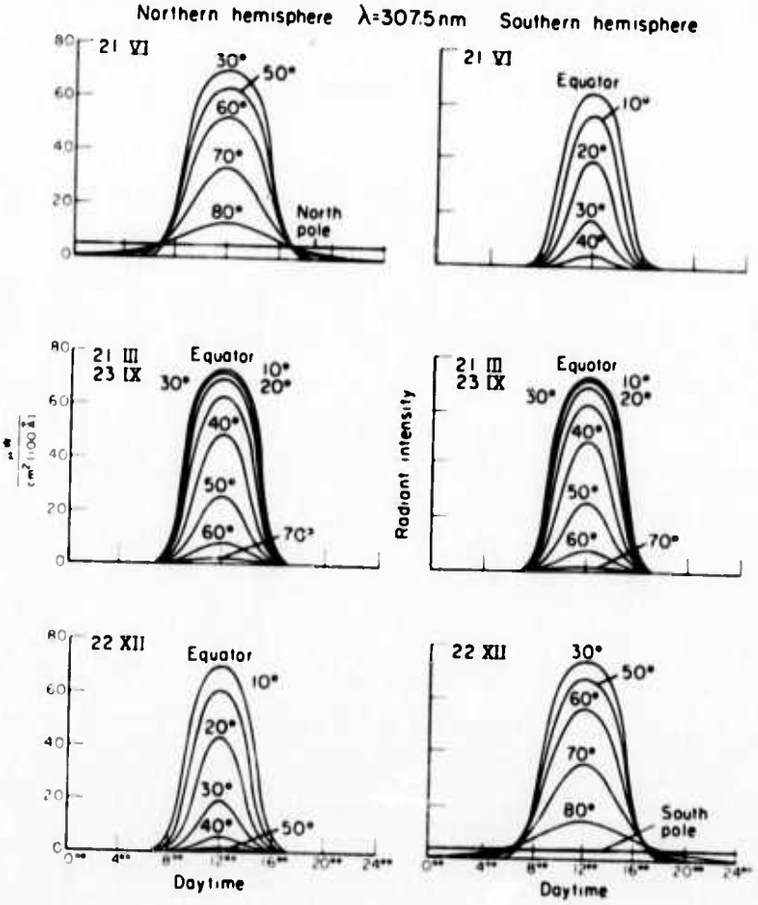

FIGURE 12. Intensity of UV Global Solar Radiation (λ = 307.5 nm) for Different Latitudes and Seasons, by Time of Day. (Source: Ref. 5.)

For the horizontal incident surface assumed in Figs. 8-12 and Table 3 no contribution is included from ground reflections. The importance of such effects is strikingly illustrated by Fig. 14 (Ref. 5), wherein the UV-B radiation at Davos in winter was found to exceed that in summer as a result of snow reflections from the surrounding mountains. A person standing on a beach receives reflected radiation from water and sand, a city dweller from nearby buildings, etc. Clearly, the actual incident UV radiation is not only a function of sun and atmosphere but of complex topographical parameters as well.

TABLE 3. MONTHLY SUMS OF UV RADIATION AT 307.5 nm (λ = 10 Å), ASSUMING CLOUDLESS DAYS

($w\text{-sec cm}^{-2}\ \text{month}^{-1}$)

	Jan.	Feb	Mar	Apr	May	June	July	Aug	Sept	Oct	Nov	Dec	Year
North pole	–	–	–	0.06	0.3	0.8	0.4	0.08	–	–	–	–	1.6
80°	–	–	0.01	0.3	0.8	1.2	1.0	0.4	0.06	–	–	–	3.8
70°	–	0.01	0.1	0.8	1.7	2.2	2.0	1.0	0.3	0.05	–	–	8.2
60°	0.01	0.07	0.4	1.7	2.8	3.5	3.2	1.9	0.9	0.2	0.02	–	14.7
50°	0.09	0.3	1.2	2.8	4.0	4.5	4.3	3.1	1.8	0.7	0.2	0.06	23.1
40°	0.4	1.0	2.3	3.8	4.8	5.2	5.0	4.1	2.9	1.3	0.6	0.3	31.7
30°	1.1	2.0	3.3	4.6	5.3	5.5	5.4	4.8	3.9	2.4	1.4	1.0	40.7
20°	2.2	3.1	4.3	5.0	5.4	5.5	5.4	5.2	4.6	3.5	2.4	2.0	48.7
10°	3.5	4.2	5.0	5.1	5.1	4.9	5.0	5.2	5.0	4.4	3.7	3.3	54.4
Equator	4.6	4.9	5.2	4.8	4.5	4.2	4.2	4.8	5.0	5.0	4.7	4.5	56.4
10°	5.4	5.3	5.2	4.2	3.6	3.1	3.3	4.1	4.7	5.2	5.3	5.4	54.8
20°	5.8	5.3	4.7	3.3	2.4	1.9	2.1	3.1	4.1	5.1	5.5	5.9	49.2
30°	5.9	5.0	4.0	2.1	1.3	0.9	1.0	2.0	3.2	4.6	5.4	6.0	41.4
40°	5.4	4.3	2.9	1.2	0.5	0.3	0.4	1.0	2.0	3.7	4.8	5.7	32.2
50°	4.6	3.3	1.8	0.5	0.1	0.07	0.08	0.4	1.1	2.7	4.0	4.0	23.6
60°	3.5	2.1	0.8	0.1	0.02	–	0.01	0.07	0.4	1.5	2.8	3.8	15.1
70°	2.2	1.1	0.3	0.01	–	–	–	0.05	0.09	0.7	1.7	2.5	8.7
80°	1.1	0.4	0.06	–	–	–	–	–	0.01	0.2	0.7	1.3	3.8
South pole	0.4	0.1	–	–	–	–	–	–	–	0.04	0.3	0.8	1.6

Source: Computed in Ref. 5 from values measured by Bener of Davos, Switzerland.

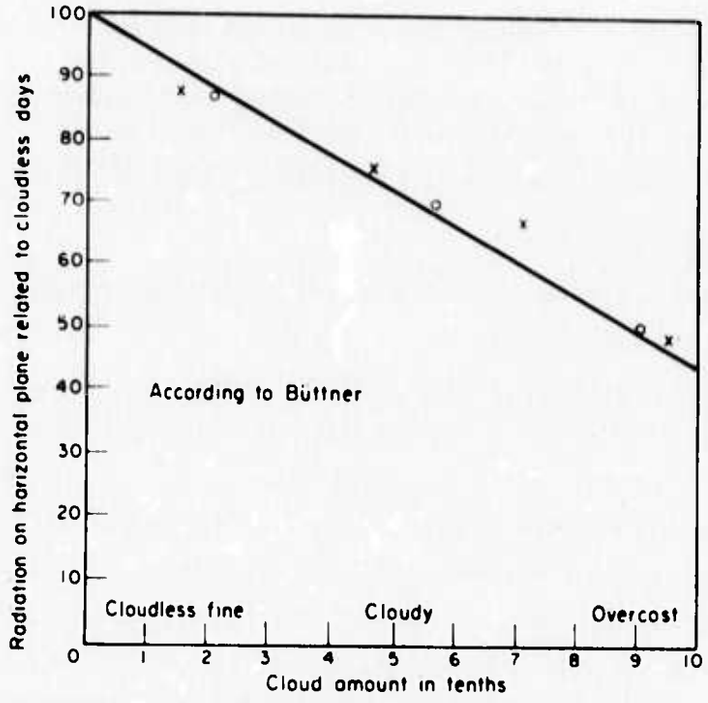

FIGURE 13. Relative Intensity of UV-B Global Solar Radiation Dependent on Cloudiness. (Source: Refs. 5,16.)

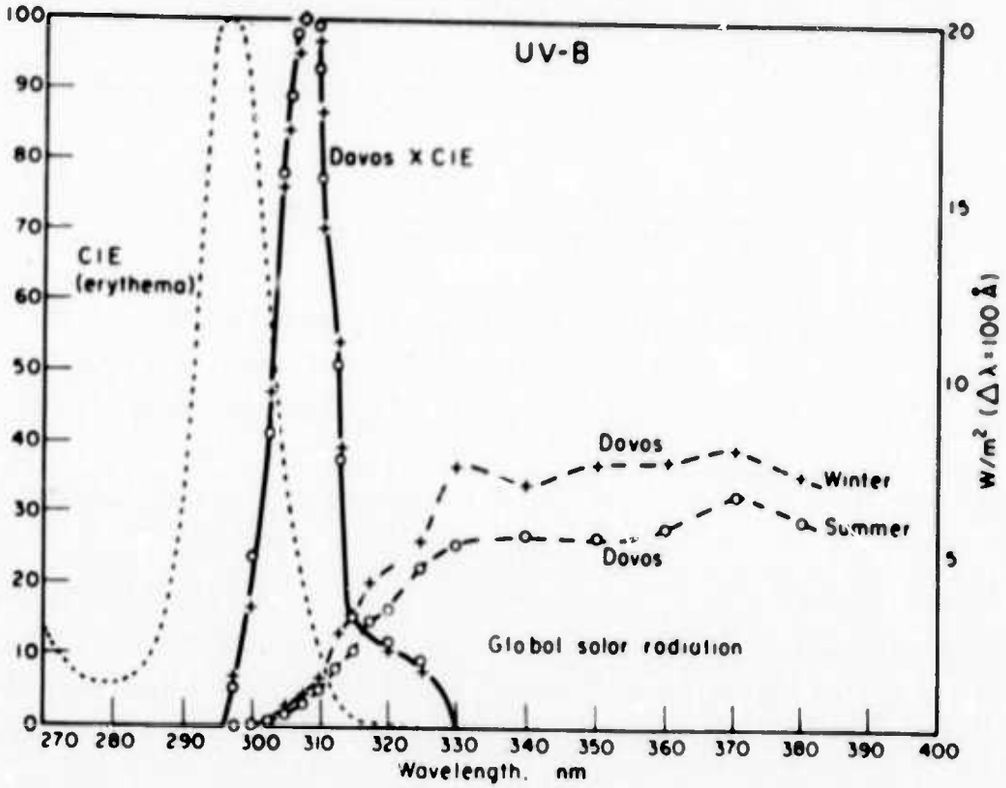

FIGURE 14. Curves of Erythemal Efficiency according to Commission Internationale de l'Eclairage (CIE) (dotted line), UV Global Solar Radiation Measured in Davos by Bener (dashed lines), and their Product (Davos x CIE) (solid line). (Source: Ref. 5.)

The fact that a person is three-dimensional introduces yet another order of complexity to any calculation of the absolute UV dose that he receives, inasmuch as every part of his body receives a different dose which depends not only on orientation with respect to the sun at some instant of time but also on the motion history of the part and its protective covering or lack thereof, the amount of exposure to the sun, etc. Fortunately, all of these complicating factors, which, of course, would vary from person to person, are not present in determining the factor increase in the average UV radiation a person would receive (Section VI) due to a specified percentage decrease in the amount of ozone, assuming his exposure habits remain unchanged.

VI. INCREASE IN ULTRAVIOLET RADIATION

Let the direct solar UV radiation flux, as represented by Eq. 4, be reduced to a level $I(\lambda, x', \theta)$ because of a decrease in the amount of ozone from x to x′. Then

$$I(\lambda, x', \theta) = I_0(\lambda)\, e^{-A(\lambda)\, x' \sec\theta - \tau_r(\lambda) \sec\theta}, \qquad (5)$$

where the Rayleigh scattering optical thickness $\tau_r(\lambda)$ will remain virtually unchanged, since ozone is a very minor constituent of the atmosphere and nearly all of the Rayleigh scattering in the beam occurs in the dense troposphere below the ozone layer (Ref. 3).

For a decrease in atmospheric ozone, the factor increase in UV radiation flux is given by the flux ratio

$$\frac{I(\lambda, x', \theta)}{I(\lambda, x, \theta)} = e^{-A(x' - x) \sec\theta}$$

$$= e^{Ax\left(1 - \frac{x'}{x}\right) \sec\theta}, \qquad (6)$$

where $\left(1 - \frac{x'}{x}\right)$ is the fractional decrease in the amount of ozone. This factor times the UV flux for some given initial total amount of atmospheric ozone gives the total amount of UV flux for some specified percentage decrease in the amount of ozone.

In Figs. 15-18 the factor increase in UV flux is plotted as a function of percentage decrease in total amount of ozone, with wavelength as a parameter, for solar zenith angles of 0°, 30°, 60°, and 75°, respectively, 0.341 atm-cm of total ozone, and $A = 10\ cm^{-1}$. Note that the factor increase can be very great for the lower wavelengths, e.g., an order of magnitude increase at $\lambda = 297.5$ nm for $\theta = 30^\circ$ and 45% ozone depletion (Fig. 16). However, this effect is

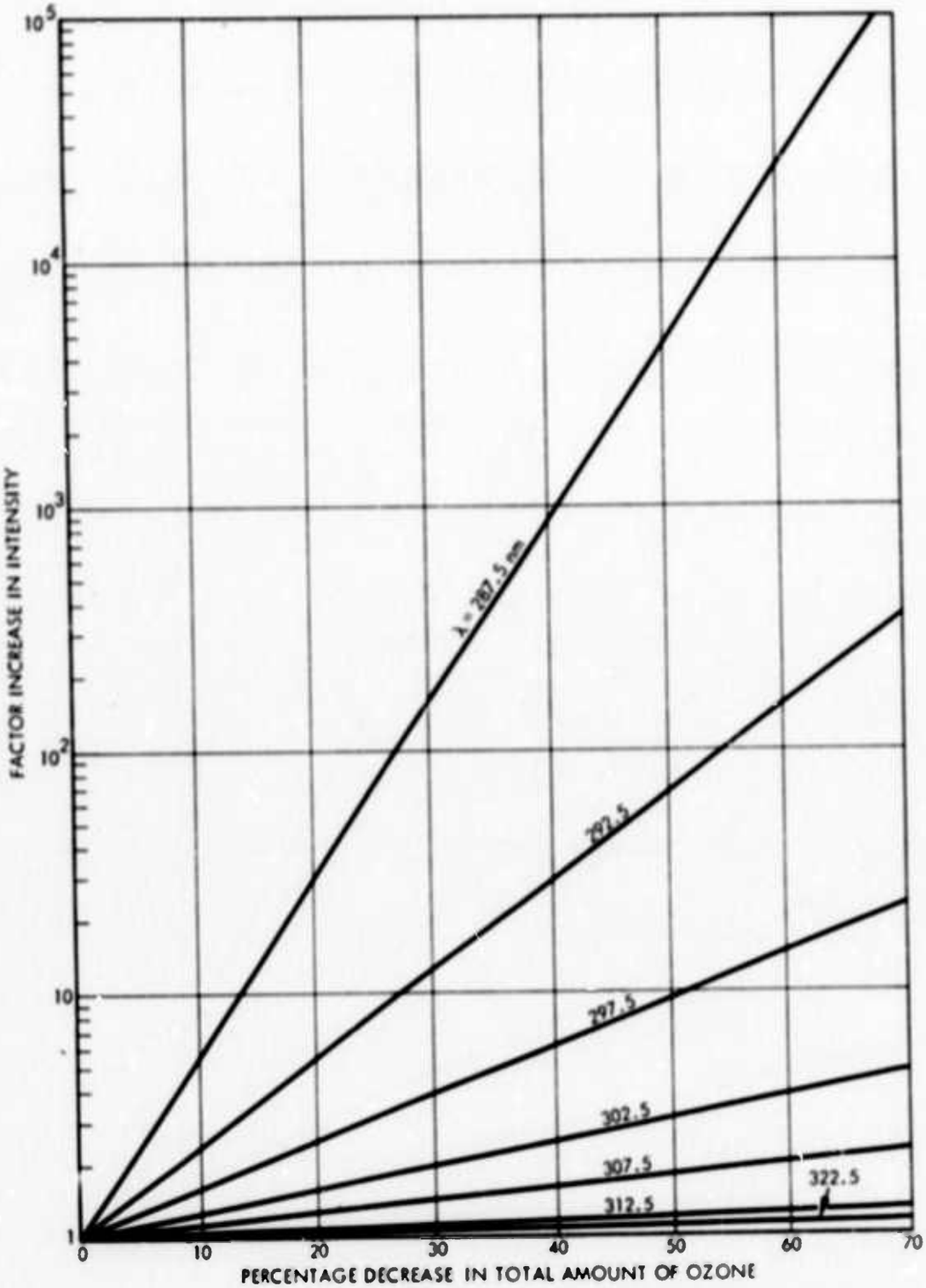

FIGURE 15. Factor Increase in Direct Solar UV Radiation Intensity versus Percentage Decrease in Total Amount of Ozone for Solar Zenith Angle θ of 0° and 0.341 atm-cm of Total Ozone.

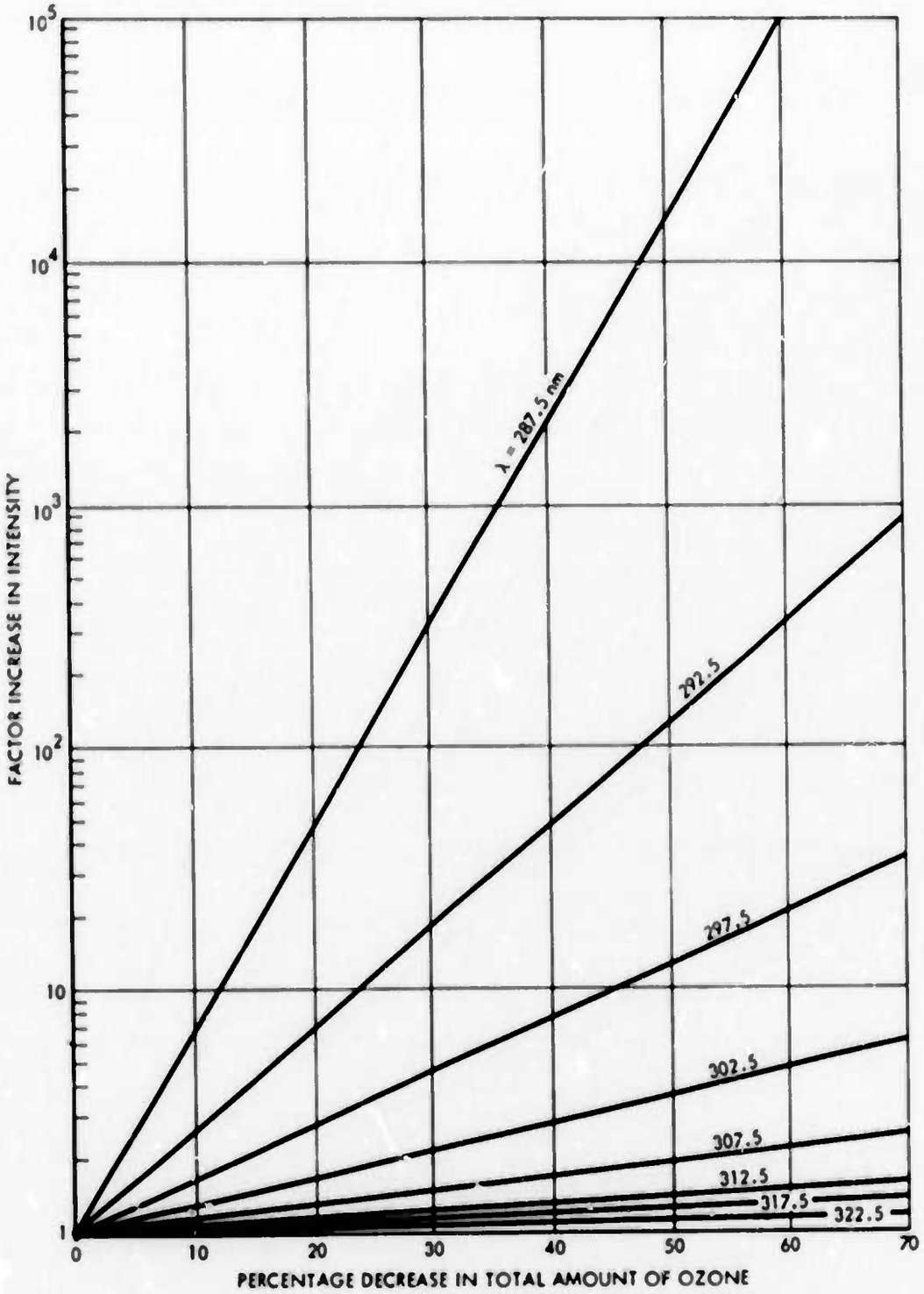

FIGURE 16. Factor Increase in Direct Solar UV Radiation Intensity versus Percentage Decrease in Total Amount of Ozone for Solar Zenith Angle θ of 30° and 0.341 atm-cm of Total Ozone.

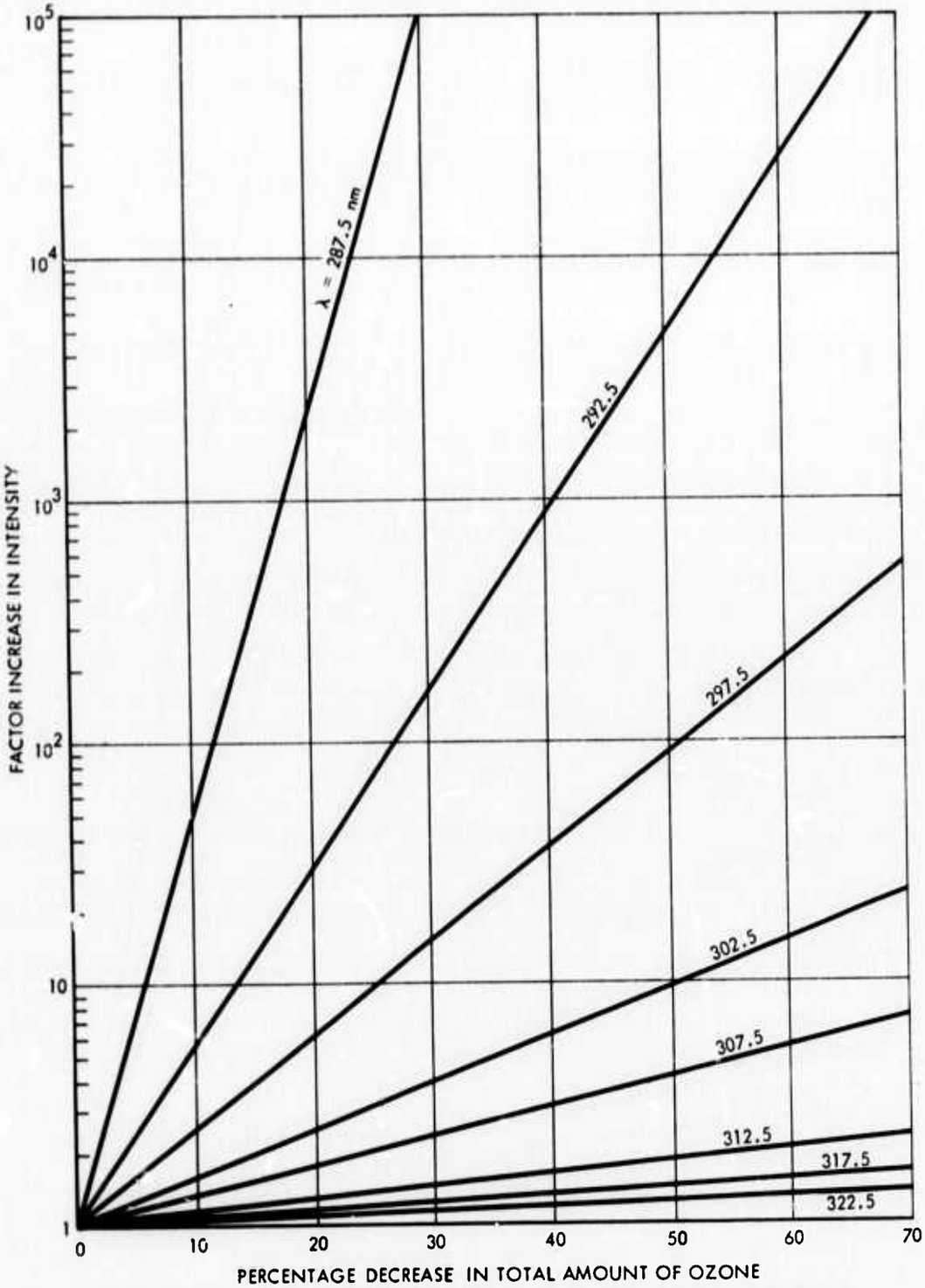

FIGURE 17. Factor Increase in Direct Solar UV Radiation Intensity versus Percentage Decrease in Total Amount of Ozone for Solar Zenith Angle θ of 60° and 0.341 atm-cm of Total Ozone.

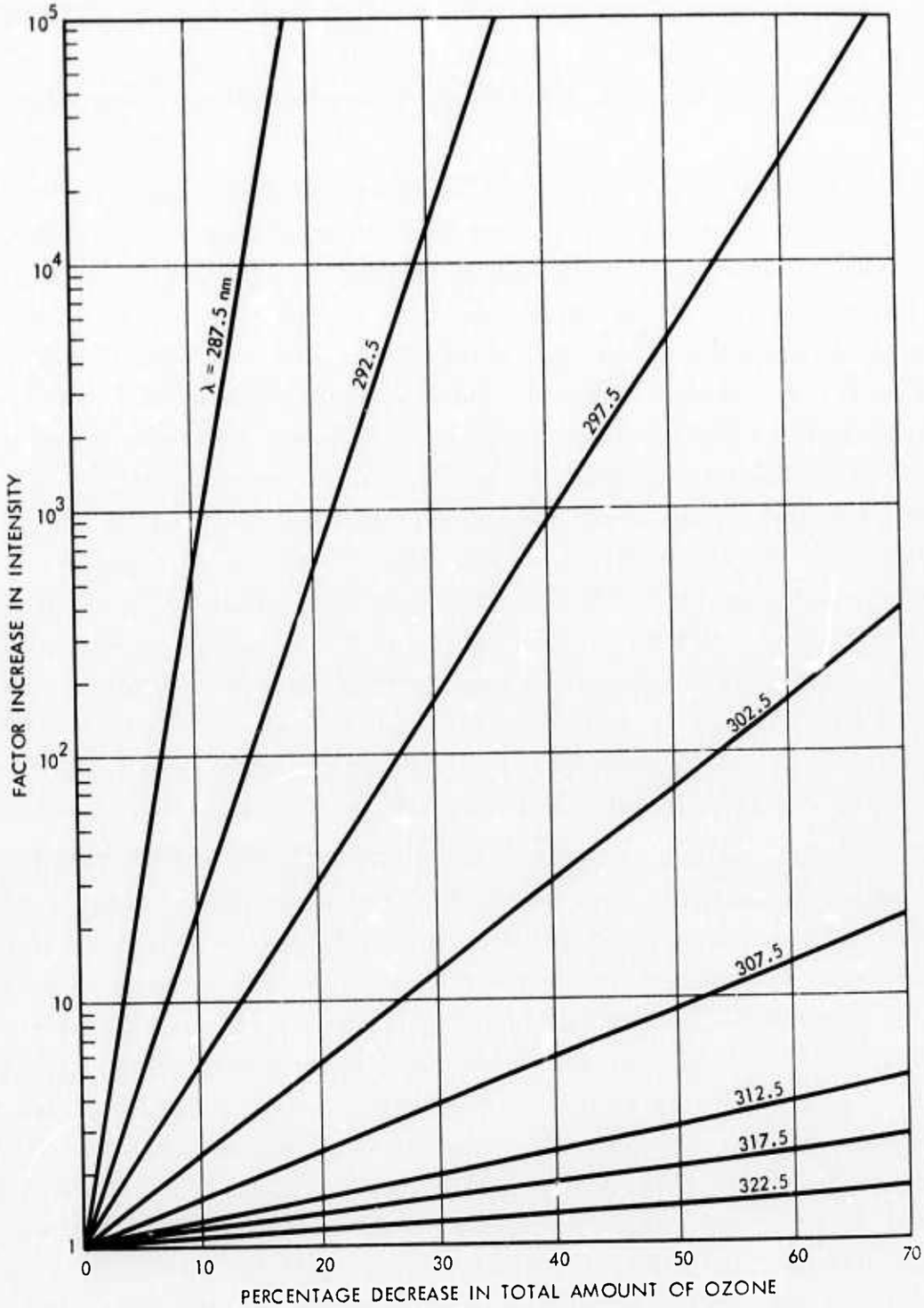

FIGURE 18. Factor Increase in Direct Solar UV Radiation Intensity versus Percentage Decrease in Total Amount of Ozone for Solar Zenith Angle θ of 75° and 0.341 atm-cm of Total Ozone.

alleviated by the fact that the direct solar UV radiation flux is less intense by a factor of 40 than at λ = 307.5 nm (Fig. 9), at which wavelength the factor increase is approximately 2.

From Figs. 15-18 it is apparent that the factor increase in direct solar UV radiation is much greater for large solar zenith angles and hence will be greater at the higher latitudes. Here again, however, this effect is counterbalanced by the greatly reduced flux levels at the higher latitudes, as is illustrated by Fig. 19. Here the noon direct irradiance at a wavelength of 297.5 nm is plotted versus latitude for the northern hemisphere in the spring. Values of ozone amount as a function of latitude were obtained from Fig. 1. It is seen that the effect of a 10% ozone depletion is to shift the present 297.5-nm noon irradiance level approximately 3° to the north for a 10% ozone depletion for latitude of 40° N., and approximately 16° to the north for a 50% ozone depletion. At the equator the corresponding shifts are approximately 13° and 36° for 10% and 50% ozone depletion, respectively. The magnitude of these shifts decreases with increasing wavelength, and, since the predominant transmitted erythemal radiation lies at the higher wavelengths, the shifts for equal erythemal dose would be far smaller than those for λ = 297.5 nm.

Figures 15-18 are also usable to determine any possible decrease in direct solar UV radiation due to a percentage increase in total ozone by reading the abscissa as the percentage increase and the ordinate as the ratio of the original to final flux values. Moreover, it is also possible to use these figures for determining the factor increase F due to a change from an arbitrary amount of total ozone x_1 to an amount of total ozone x_2 by comparing the factor increases relative to the plotted 0.341 atm-cm of ozone. Thus, if f_1 is the factor increase for x_1 compared to 0.341 atm-cm of ozone, and if f_2 is the factor increase for x_2 compared to 0.341 atm-cm of ozone, the factor increase $f_{1,2}$ for x_1 compared to x_2 is simply given by

$$f_{1,2} = \frac{f_2}{f_1} . \qquad (7)$$

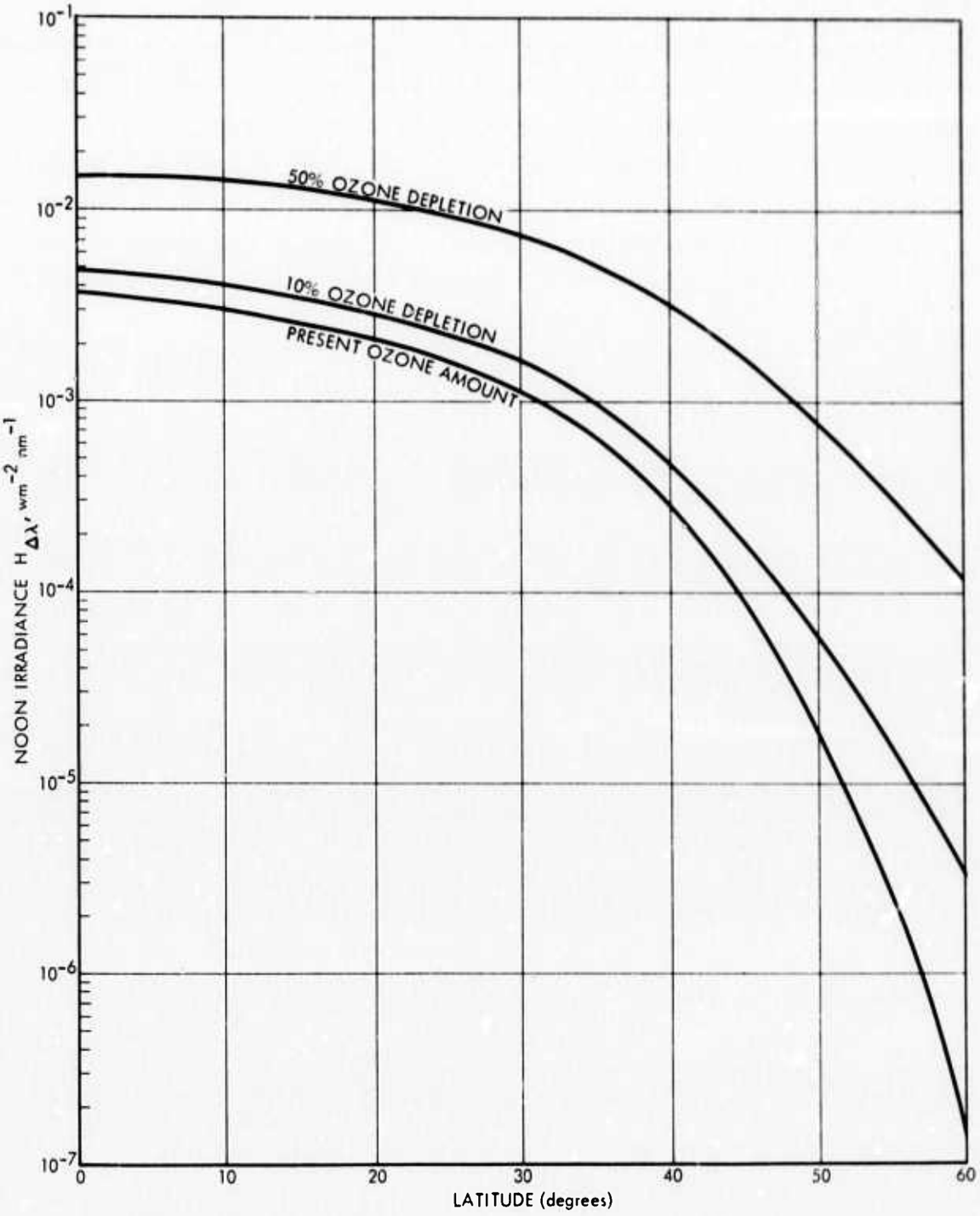

FIGURE 19. Noon Direct Irradiance at λ = 297.5 nm Versus Latitude for Northern Hemisphere in the Spring

Unfortunately, Figs. 15-18 for determining the changes in direct solar UV radiation do not apply for scattered diffuse sky radiation. In Ref. 7, the calculations apply to but a single amount of ozone, 0.341 atm-cm, and a single distribution of ozone with altitude. The computer program divides the atmosphere into 366 layers to obtain the desired accuracy. The program is available at NASA Goddard Space Flight Center for calculations involving different ozone parameter values.

VII. INCREASE IN ERYTHEMAL DOSE

As an example of the biological impact that an increase in UV radiation could have, the increase in erythemal radiation has been calculated for several specific cases. If the radiation response spectrum for other biological organisms such as plants is known, the procedure described below may be similarly applied.

Let $E(\lambda)$ denote the erythemal response curve, normalized to a value of unity at $\lambda = 297.5$ nm, as shown in Fig. 14 and tabulated in Table 4. If $H_{\Delta\lambda}$ is the current solar UV radiation in w m^{-2} nm^{-1} and $F(\lambda)$ the factor increase in intensity, the erythemal dose D is given by

$$D = \int_{\lambda} E(\lambda) H_{\Delta\lambda}(\lambda)\, F(\lambda)\, d\lambda \qquad (9)$$

In Table 4 the above factors are given at 1-nm intervals for $\theta = 30^{\circ}$, 50% ozone depletion, and 0.341 atm-cm of ozone. The $F(\lambda)$ function is here applied to the sum of the direct and scattered radiation, although it must be recognized that it is strictly valid only for direct radiation. The numerical integration results in a tripling of the erythemal dose for these particular parameters. It is also important to note that the peak of the erythemal dose curve has shifted downward from 307.5 nm (Fig. 14) to 301.5 nm (Fig. 20). The integrand in Eq. 9 is plotted in Fig. 20 for $\theta = 30^{\circ}$ and $\theta = 60^{\circ}$. In the latter case, the erythemal dose is increased by a factor of 4½, but it is seen that even this increase would not bring the erythemal dose up to the 0.341 atm-cm reference level for $\theta = 30^{\circ}$. These two results are characteristic of doses that could be expected at noon over North America in spring at a latitude of 30° and in fall at a latitude of 60°.

A similar calculation of increased erythemal dose for a 10% reduction in ozone resulted in a much less alarming 23% increase in erythemal dose for $\theta = 30^{\circ}$.

TABLE 4. FACTOR INCREASE IN ERYTHEMAL DOSE FOR $\theta = 30^{\circ}$ AND 50% OZONE DEPLETION, ASSUMING 0.341 atm-cm INITIAL OZONE

λ, nm	E	$H_{\Delta\lambda}$, w $m^{-2}nm^{-1}$	Equivalent $H_{\Delta\lambda}$ at 297.5 nm	$F(\lambda)$ Factor Increase in $H_{\Delta\lambda}$	Equivalent $H_{\Delta\lambda}$ at 297.5 nm with 50% Ozone Depletion
287.5	0.13	4×10^{-10}	--	1.5×10^{4}	--
288.5	0.18	3×10^{-9}	--	--	--
289.5	0.22	3×10^{-8}	--	--	--
290.5	0.33	2×10^{-7}	--	--	--
291.5	0.44	1.5×10^{-6}	--	--	--
292.5	0.55	10^{-5}	--	120	0.0007
293.5	0.66	4×10^{-5}	--	80	0.0021
294.5	0.77	1.2×10^{-4}	0.0001	50	0.0046
295.5	0.88	2.8×10^{-4}	0.0002	30	0.0074
296.5	0.98	6×10^{-4}	0.0006	20	0.0118
297.5	1.00	1.2×10^{-3}	0.0012	12.5	0.0150
298.5	0.98	2.5×10^{-3}	0.0024	10	0.0245
299.5	0.88	4.5×10^{-3}	0.0040	8	0.0317
300.5	0.77	7.5×10^{-3}	0.0058	6	0.0346
301.5	0.66	0.012	0.0079	5	0.0396
302.5	0.55	0.018	0.0099	3.6	0.0356
303.5	0.44	0.026	0.0114	3	0.0343
304.5	0.33	0.035	0.0115	2.8	0.0323
305.5	0.22	0.047	0.0103	2.5	0.0258
306.5	0.18	0.063	0.0113	2.2	0.0249
307.5	0.14	0.080	0.0112	1.9	0.0213
308.5	0.12	0.100	0.0120	1.8	0.0216
309.5	0.10	0.125	0.0125	1.7	0.0212
310.5	0.08	0.150	0.0120	1.6	0.0192
311.5	0.05	0.170	0.0085	1.5	0.0128
312.5	0.03	0.190	0.0057	1.4	0.0080
			0.1385		0.4290

Factor Increase in Erythemal Dose: 3

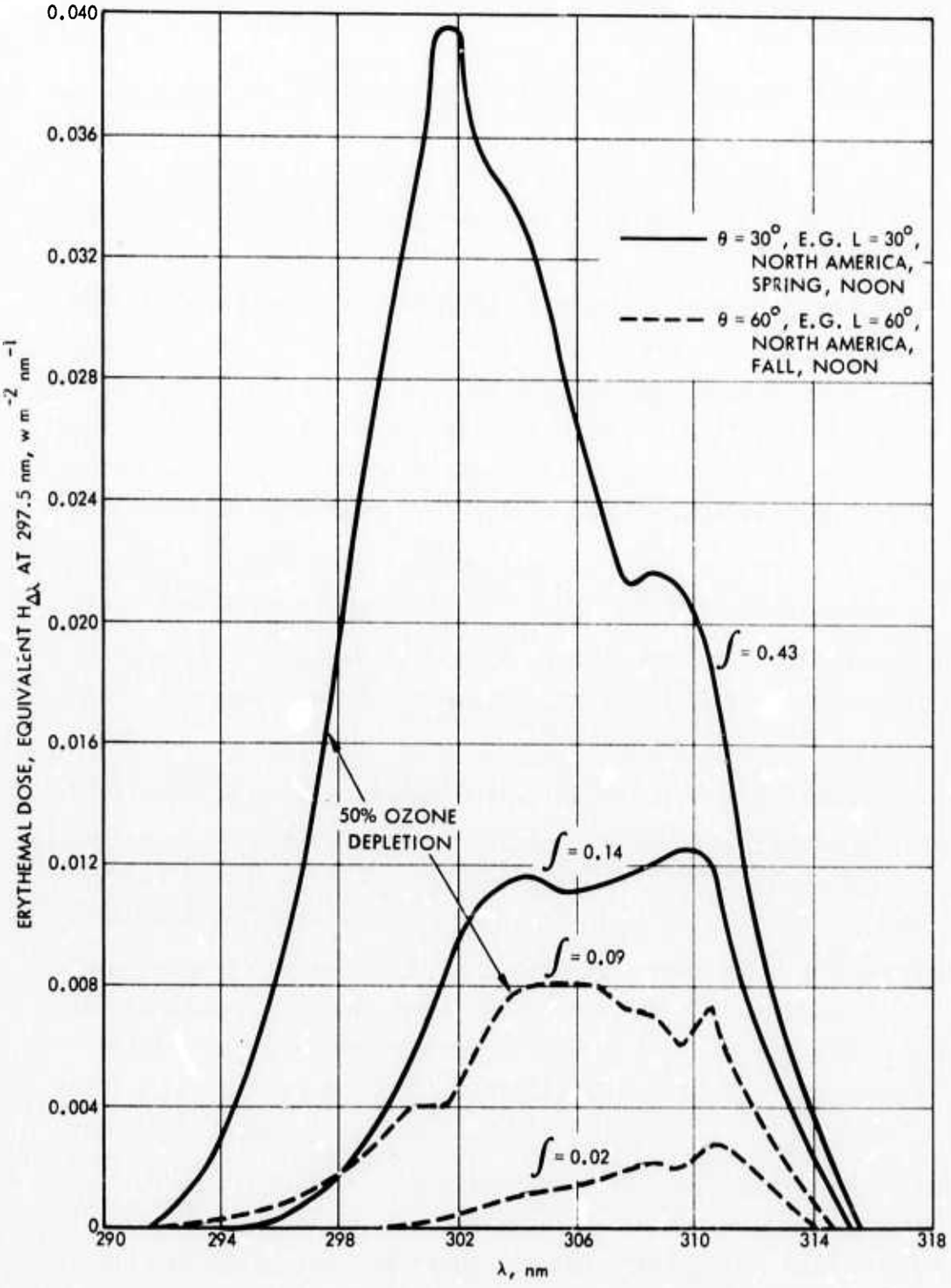

FIGURE 20. Effect of 50% Ozone Depletion on Erythemal Dose.

VIII. CONCLUSIONS

1. While there are daily, monthly, and annual fluctuations in the amount of ozone which could well exceed the amount of ozone depleted by a fleet of 500 SSTs, a man-made depletion would be a unidirectional variation, resulting in a lowering of the mean amounts of ozone and hence increasing the amount of average worldwide UV radiation incident on the surface of the Earth.

2. For solar zenith angles exceeding about 30°, direct solar UV radiation will be exceeded by scattered sky UV radiation.

3. UV radiation on Earth is a decreasing function of latitude because of increasing solar zenith angle and increasing amount of ozone.

4. UV radiation in the biologically important spectral region decreases very sharply with decreasing wavelength due to the exponential behavior of the ozone absorption coefficient in this region (280-320 nm).

5. The factor increase in UV radiation resulting from a depletion in the amount of ozone will be greatest for the biologically harmful lower wavelengths and at the higher latitudes. Fortunately, for these conditions the intensity of UV radiation is very weak (Items 3 and 4).

6. Determination of the factor increase in direct solar radiation due to a depletion in the amount of ozone is a mathematically simple problem; for scattered sky radiation it is not. However, a computer program is available at Goddard Space Flight Center which can solve this complex problem for any set of prescribed

conditions. Presently available data are for 0.341 atm-cm of ozone and a specified ozone altitude profile.

7. For a solar angle of 30^{o} and 0.341 atm-cm of ozone, the erythemal dose would be approximately tripled if there were to be a 50% depletion in the amount of ozone; for a 10% depletion there would be a 23% increase in erythemal dose. For the case of 50% ozone depletion, the peak of the erythemal dose curve is shifted downward from 307.5 nm to 301.5 nm.

REFERENCES

1. H. Johnston, "Reduction of Stratospheric Ozone by Nitrogen Oxide Catalysts from Supersonic Transport Exhaust," Science, Vol. 173, 6 August 1971.

2. B. E. Johnson, F. Daniels, Jr., and I. A. Magnus, "Response of Human Skin to Ultraviolet Light," Photophysiology, Vol. 4, 1968.

3. Air Force Cambridge Research Laboratories, Office of Aerospace Research, United States Air Force, Handbook of Geophysics and Space Environment, Bedford, Mass., 1965.

4. Air Force Cambridge Research Laboratories, Office of Aerospace Research, United States Air Force, Ozonesonde Observations over North America, Vol. 2, Environmental Research Papers No. 38, Meteorology Project 9631, Bedford, Mass., 1964.

5. R. Schulze and K. Gräfe, "Consideration of Sky Ultraviolet Radiation in the Measurement of Solar Ultraviolet Radiation," The Biologic Effects of Ultraviolet Radiation, F. Urbach, ed., Pergamon Press, New York, 1969.

6. H. S. Willet, "The Relationship of Total Atmospheric Ozone to the Sunspot Cycle," J. Geophys. Res., Vol. 67, No. 2, February 1962.

7. J. V. Dave and P. M. Furukawa, "Scattered Radiation in the Ozone Absorption Bands at Selected Levels of a Terrestrial Rayleigh Atmosphere," Meteorological Monographs, Vol. 7, No. 29, January 1966.

8. E. C. Y. Inn and Y. Tanaka, "Absorption Coefficient of Ozone in the Ultraviolet and Visible Regions," J. Opt. Soc. Am., Vol. 43, No. 10, October 1953.

9. M. Griggs, "Absorption Coefficients of Ozone in the Ultraviolet and Visible Regions," J. Chem. Phys., Vol. 49, No. 2, 15 July 1968.

10. P. Bener, "Spectral Intensity of Natural Ultraviolet Radiation and its Dependence on Various Parameters," The Biologic Effects of Ultraviolet Radiation, F. Urbach, ed., Pergamon Press, New York, 1969.

11. Kendric C. Smith, "Biochemical Effects of Ultraviolet on DNA," The Biological Effects of Ultraviolet Radiation, F. Urbach, ed., Pergamon Press, New York, 1969.

12. Arthur C. Giese, "Effects of Ultraviolet Radiations on Some Activities of Animal Cells," The Biological Effects of Ultraviolet Radiation, F. Urbach, ed., Pergamon Press, New York, 1969.

13. Goddard Space Flight Center, National Aeronautics and Space Administration, The Solar Constant and the Solar Spectrum Measured from a Research Aircraft, N70 42638, M. P. Thekaekara, October 1970.

14. F. S. Johnson, "The Solar Constant," J. Meteorol., Vol. 11, No. 6, December 1954.

15. C. R. Detweiler, D. L. Garrett, J. D. Purcell, and R. Tousey, "The Intensity Distribution in the Ultraviolet Solar Spectrum," Annales de Geophysique, Vol. 17, No. 3, July-September 1961.

16. K. Büttner, Physik. Bioklimat., Leipzig, 1938; H. Pfliderer and K. Büttner, Bioklimatologie, Lehrbuch für Bäder- und Klimaheilkunde, 1940.

APPENDIX

EFFECT OF INJECTION OF NO_x ON OZONE CONCENTRATION

The question of the ozone depletion that can be expected from a fleet of SST aircraft has not been resolved at the present time, and arguments on the subject are continuing. A study by Johnston (Ref. A-1) postulates the ozone profiles as shown in Fig. 20, Panels A-D, for a fleet of 500 SST aircraft (334 with four engines each and 166 with two engines each), with each SST cruising in the stratosphere for 7 hours per day. In Fig. A-1, Panels E-H, a dose of NO_x ten times higher was assumed than might be expected over the heavily traveled region of the world. Thus, a 50% ozone depletion (Fig. A-1, Panel H) represents the worst case of highest dose and a uniform distribution of injected NO_x over a wide altitude band between 15 and 31 km. At the other extreme, if the altitude band could be compressed to 20-21 km, the results indicate that the reduction in the amount of ozone would be only 3%.

A recent investigation by Foley and Ruderman (Ref. A-2) has shown that during certain years of high-yield nuclear testing, a few times 10^{34} nitric oxide molecules were probably injected into the stratosphere. This is comparable to upper estimates for NO generation from 500 SSTs flying for a year. It was concluded that the postulated large catalytic ozone reduction from such NO injection is not supported by worldwide or local total ozone measurements. However, Johnston et al. (Ref. A-3) countered that on thermodynamic grounds the Foley-Ruderman estimates of NO_x production were too high and that their estimates of the mass of hot air produced were also too high.

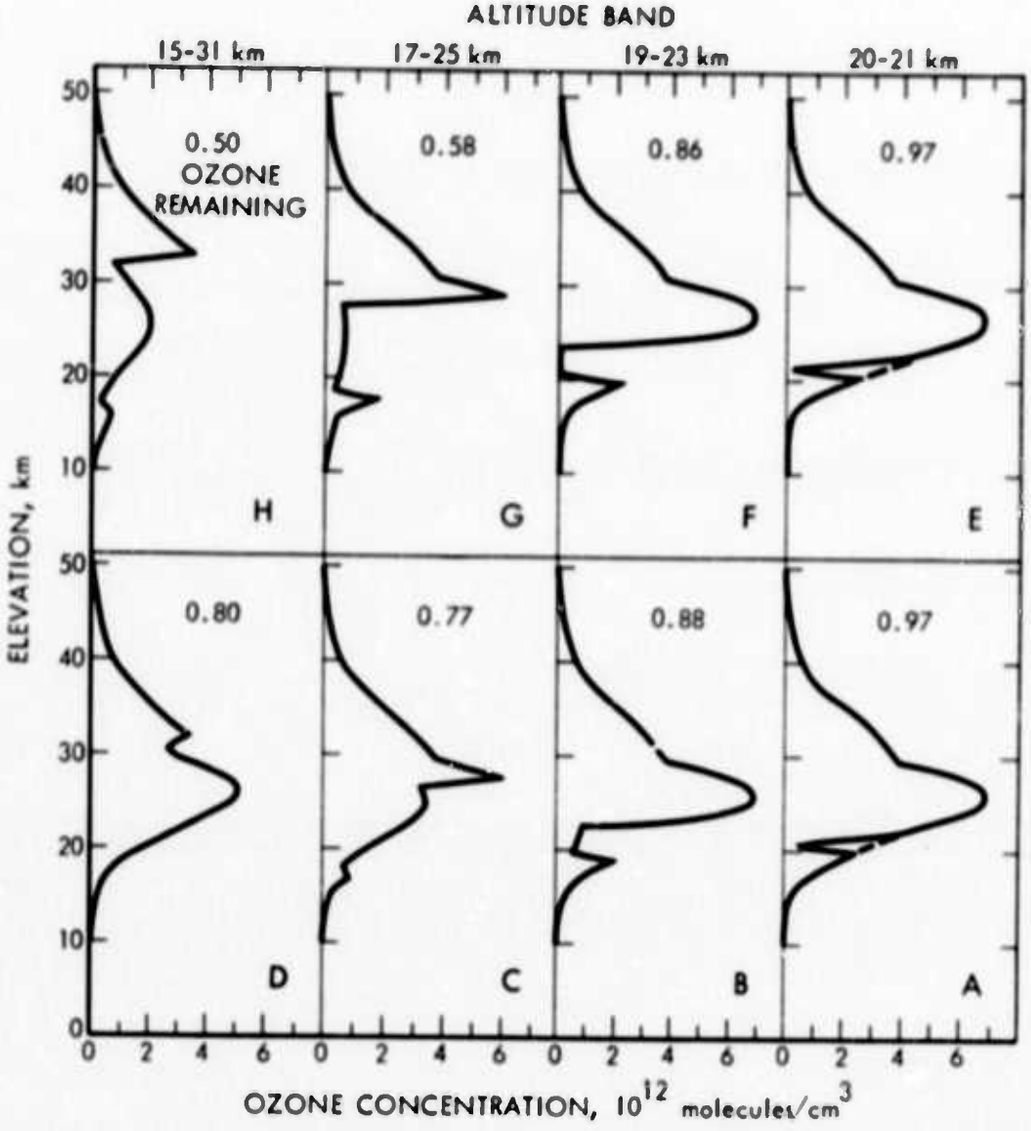

FIGURE A-1. Effect of Injection of NO_x on Ozone Concentration. (Source: Ref. A-2.)

REFERENCES

A-1. H. Johnston, "Reduction of Stratospheric Ozone by Nitrogen Oxide Catalysts from Supersonic Transport Exhaust," Science, Vol. 173, August 6, 1971.

A-2. Institute for Defense Analyses, Stratospheric NO Production from Past Nuclear Explosions and its Relevance to Projected SST Pollution, IDA (JASON) Paper P-894, H. Foley and M. Ruderman, August 1972.

A-3. University of California, The Effect of Nuclear Explosions on Stratospheric NO and O_3, LBL-1421, H. S. Johnston, G. Whitten, and J. Berks, October 1972.